Title

Vampire Worms; A revision of Galapagomystides (Phyllodocidae, Annelida), with the description of three new species.

Author

Pearson, Kaila Ann Marjorie

Publication Date

2021

Peer reviewed|Thesis/dissertation

UNIVERSITY OF CALIFORNIA SAN DIEGO

Vampire Worms; A revision of *Galapagomystides* (Phyllodocidae, Annelida), with the description of three new species.

A thesis submitted in partial satisfaction of the requirements
for the degree Master of Science

in

Marine Biology

by

Kaila Pearson

Committee in charge:

Professor Greg Rouse, Chair
Professor Nicholas Holland
Professor Deirdre Lyons

2021

The thesis of Kaila Pearson is approved, and it is acceptable in quality and form for publication on microfilm and electronically.

University of California San Diego

2021

TABLE OF CONTENTS

LIST OF FIGURES

LIST OF TABLES

ACKNOWLEDGEMENTS

I would like to acknowledge Dr. Greg Rouse for his advice and support as the chair of my committee. Not only did Dr. Greg Rouse guide me through several manuscript drafts, but he also equipped me with the necessary research skills and knowledge it took to complete this project.

I would also like to acknowledge my two other committee members, Dr. Nicholas Holland and Dr. Deirdre Lyons for their guidance during my project.

I want to thank my family and friends for their support during my time in graduate school. I especially want to express gratitude to my father, Bob Pearson, my mother, Kathy Pearson, my partner, Patrick Shaughnessy, and my grandmother Marge Pearson; their guiding light is immeasurable and so valued.

This manuscript is coauthored with Dr. Greg Rouse. The thesis author was the primary author of this manuscript.

ABSTRACT OF THE THESIS

Vampire Worms; A revision of *Galapagomystides* (Phyllodocidae, Annelida), with the description of three new species.

By
Kaila Pearson
Master of Science in Marine Biology
University of California San Diego, 2021
Professor Greg Rouse, Chair

Galapagomystides is an exclusively deep sea group of phyllodocid annelids, originally erected for *Galapgomystides aristata* from hydrothermal vents of the Galapagos Rift. In this study, numerous specimens of Phyllodocidae collected from hydrothermal vents and methane seeps from the Pacific Ocean, including specimens that are likely to represent *Galapgomystides aristata,* were studied using morphology (light microscopy and scanning electron microscopy) and DNA sequence data. Phylogenetic analysis of the newly generated molecular data (cytochrome c oxidase subunit I, 16S rRNA, 18S rRNA, and 28S rRNA) combined with an already available extensive dataset for Phyllodocidae resulted in a monophyletic *Galapagomystides*. Two new species from hydrothermal vents in the West Pacific, *G. bobpearsoni* n. sp., and *G. kathyae* n. sp., as well as one new species from a cold

seep in the East Pacific, *G. patricki* n. sp. were inferred from the phylogenetic results and morphology. These new species are formally described, and a previously known vent species, *Protomystides verenae*, is redescribed and transferred to *Galapagomystides*. *Galapagomystides verenae* was found to occur in both vents and seeps in the eastern Pacific, from Oregon to Costa Rica. The diagnosis of *Galapagomystides* is amended and the biogeography and habitat evolution of the five species of *Galapagomystides* is discussed. This study reinforces the conception that species within the genus *Galapagomystides* likely feed on the blood of tube worms, resulting in the colloquial name applied here, “vampire worms”.
key words: deep sea, Pacific Ocean, Polychaeta, Phyllodocidae, new species

Introduction

Deep sea chemosynthetic ecosystems (vents and seeps) support diverse communities of animals (Levin 2016; Van Dover 2000) well-known animals from these habitats tend to be megafauna such as mussels (McCowin *et al.* 2020), clams (Krylova *et al.* 2010) and siboglinid tube worms such as Vestimentifera (McCowin and Rouse 2018). Despite the attention given to larger animals, less conspicuous macrofaunal and meiofaunal groups of annelids, molluscs and crustacea comprise much of the diversity at seeps and vents (Desbruyères *et al.* 2006). Among the annelids, several lineages have proliferated, while many lineages common in shallow water are rare or absent. Apart from Siboglinidae, annelid groups at vents and seeps include Polynoidae (scale worms), Dorvilleidae, and Hesionidae (Hatch *et al*. 2020; Rouse *et al.* 2018; Yen and Rouse 2020). Other groups such as Serpulidae and Phyllodocidae are present, though with much lower species richness (Blake, 1985; Rouse and Kupriyanova 2021).

Phyllodocidae is a clade of predatory annelids that contains over 500 named species, found in most marine habitats. Phyllodocidae are commonly known as ‘paddle worms’, owing to their large, flat dorsal cirri. Many taxa live nearshore in the rocky intertidal (Muir *et al*. 2014), while others live in the deep sea (Imajima, 2001). Most Phyllodocidae are benthic, with the exception of the holopelagic group Alciopini (San Martin *et al.* 2020; Rouse and Pleijel, 2001). Only a few Phyllodocidae have been recorded from chemosynthetic environments, all in the Pacific Ocean. The named species to date are *Galapagomystides aristata* Blake, 1985 from vents at the Galapagos Rift, *Protomystides papillosa* Blake, 1985 from vents at the East Pacific Rise (EPR, at 21°N), *Protomystides hatsushimaensis* Miura, 1988 from a cold-seep in Sagami Bay (Japan) and *Protomystides verenae* Blake, 1990 from vents at Juan de Fuca Ridge (off British Columbia).

Galapagomystides aristata has been documented within an aggregation of *Riftia pachyptila* (Govenar *et al.* 2004), (Govenar *et al.* 2005) and an earlier study inferred that *G. aristata* feeds on the blood of Vestimentifera based on anatomical and histological observations of specimens from the East Pacific Rise (Jenkins *et al.* 2002). An unnamed '*Protomystides'* has also been hypothesized to be a 'blood parasite' of *Escarpia laminata* tubes in the Gulf of Mexico (Becker *et al.* 2013). While the many members of Hirudinea are blood-feeders and occasionally referred to as vampire worms, it seems appropriate to also apply this common name to *Galapagomystides aristata* and its blood-feeding relatives.

The first phylogenetic analysis of Phyllodocidae was a morphological cladistic study by Pleijel (1991). The analysis showed that *Galapagomystides* was part of Eteoninae and a sister taxon to a clade comprising *Mysta*, *Hypereteone* and *Eteone*; in addition, Pleijel found that *Protomystides* was a member of Eteoninae. Subsequently there has been no phylogenetic examination of the placement of *Galapagomystides*, though there have been otherwise well-sampled molecular phylogenetic analyses (Eklöf *et al.* 2007; Leiva *et al.* 2018; San Martin *et al.* 2021) comprising many genera within the family, including a member (non-vent) of *Protomystides*.

Here, we present the first molecular sequence data for *Galapagomystides aristata, Protomystides verenae* and several other Phyllodocidae from western Pacific vents and eastern Pacifica seeps. This includes fragments of the mitochondrial cytochrome c oxidase subunit I (COI) and 16S rRNA (16S), as well as nuclear 18S rRNA (18S), and 28S rRNA (28S) sequences. These taxa are then analyzed along with available data for other Phyllodocidae. This allowed for the inference of three new species. These are formally described and *Galapagomystides aristata, Protomystides verenae* are redescribed and *Galapagomystides* is amended.

Materials and Methods

Sample Collection

Sample collection took place over several years in multiple localities shown in Table 1 and Figure 1 during research cruises using ROVs (remotely operated vehicle), or the HOV (human operated vehicle) *Alvin* in the Pacific Ocean during years 2005-2019. Samples were fixed in 95% ethanol (for DNA analysis), 5% formalin in seawater (for morphological analysis), or 1% osmium tetroxide (for SEM), and later rinsed and preserved in either 50% ethanol for the latter two methods. When there were few specimens per lot, worms were cut in half; anteriors were fixed in formalin and posteriors were preserved in ethanol. Pictures of live specimens were taken in the field, with Leica S8 APO or Leica MZ9.5 stereo microscopes and Canon EOS Rebel cameras. Phyllodocidae samples were collected from vents of the following regions; Lau Back-arc Basin, North Fiji Basin, southern East Pacific Rise (EPR), and the Juan de Fuca Ridge (Oregon). Samples were also collected from seep systems from the following regions; Hydrate Ridge (Oregon), Guaymas Basin (Mexico) and Costa Rica (Pacific). For locality details see Table 1.

Table 1. Voucher name, origin, locational coordinate, collection depth, date of collection and GenBank accession numbers of sequenced vouchers for genes; COI, 16S, 18S, 28S. Note- *Protomystides verenae* is referred to as *Galapagomystides verenae* in this table, and generally through the rest of this study.

Scientific Name	Voucher or Reference	Origin	Locational Coordinates	Depth (meters)	Dive Number	Date of Collection	COI GenBank Accession Number	16S GenBank Accession Number	18S GenBank Accession Number	28S GenBank Accession Number
Galapagomystides bobpearsoni n. sp.	SIO-BIC A4588	Tow Cam Vent, at Lau Back-arc Basin, Tonga	20.3178° S 176.1373° W	~2720	Jason II 142	May 19, 2005	MZ711262	MZ773004	MZ768998	MZ773063
Galapagomystides bobpearsoni n. sp.	SIO-BIC A4590	Tow Cam Vent, at Lau Back-arc Basin, Tonga	21.989° S 176.5682° W	~1891	Jason II 143	May 20, 2005	-	-	-	-
Galapagomystides kathyae n. sp.	SIO-BIC A13418	White Lady Vent, North Fiji Basin	16.9905° S 173.9147° E	~1990	Jason II 153	June 1, 2005	MZ711261	-	MZ768997	MZ773062
Galapagomystides kathyae n. sp.	SIO-BIC A13422	White Lady Vent, North Fiji Basin	16.9905° S 173.9147° E	~1990	Jason II 153	June 1, 2005	-	-	-	-
Galapagomystides kathyae n. sp.	SIO-BIC A13423	White Lady Vent, North Fiji Basin	16.9905° S 173.9147° E	~1990	Jason II 153	June 1, 2005	-	-	-	-
Galapagomystides kathyae n. sp.	SIO-BIC A13424	White Lady Vent, North Fiji Basin	16.9905° S 173.9147° E	~1990	Jason II 153	June 1, 2005	-	-	-	-
Galapagomystides kathyae n. sp.	SIO-BIC A4651	White Lady Vent, North Fiji Basin	16.9907° S 173.915° E	~1990	Jason II 152	May 31, 2005	-	-	-	-
Galapagomystides kathyae n. sp.	SIO-BIC A4645	White Lady Vent, North Fiji Basin	16.9908° S 173.915° E	~1990	Jason II 151	May 30, 2005	-	-	-	-
Galapagomystides kathyae n. sp.	SIO-BIC A4587	Tow Cam Vent, at Lau Back-arc Basin, Tonga	20.3178° S 176.1373° W	~2720	ROV Jason II	May 19, 2005	-	-	-	-
Galapagomystides patricki n. sp.	SIO-BIC A13419	Parrita Seep, Costa Rica	9.0303° N 84.623° W	~1415	AD4508	March 1, 2009	MZ711314	MZ773005	MZ768999	MZ773064
Galapagomystides patricki n. sp.	SIO-BIC A13420	Parrita Seep, Costa Rica	9.0303° N 84.623° W	~1415	AD4508	March 1, 2009	MZ711315	-	-	-
Galapagomystides patricki n. sp.	SIO-BIC A13421	Parrita Seep, Costa Rica	9.0303° N 84.623° W	~1415	AD4508	March 1, 2009	MZ711316	-	-	-
Galapagomystides patricki n. sp.	SIO-BIC A13425	Parrita Seep, Costa Rica	9.0303° N 84.623° W	~1415	AD4508	March 1, 2009	-	-	-	-
Galapagomystides patricki n. sp.	SIO-BIC A13426	Parrita Seep, Costa Rica	9.0303° N 84.623° W	~1415	AD4508	March 1, 2009	-	-	-	-
Galapagomystides patricki n. sp.	SIO-BIC A13427	Parrita Seep, Costa Rica	9.0303° N 84.623° W	~1415	AD4508	March 1, 2009	-	-	-	-
Galapagomystides patricki n. sp.	SIO-BIC A9964	Parrita Seep, Costa Rica	9.0318° N 84.6205° W	~1400	AD4990	Nov. 5, 2018	MZ711320	-	-	-
Galapagomystides patricki n. sp.	SIO-BIC A9875	Parrita Seep, Costa Rica	9.0318° N 84.6206° W	~1400	AD4990	Nov. 5, 2018	MZ711317	-	-	-
Galapagomystides patricki n. sp.	SIO-BIC A9877	Parrita Seep, Costa Rica	9.0318° N 84.6206° W	~1400	AD4990	Nov. 5, 2018	MZ711318	-	-	-
Galapagomystides patricki n. sp.	SIO-BIC A9947 (MZUCR)	Jaco Scar, Costa Rica	9.1176° N 84.8407° W	~1762	AD4989	Nov. 4, 2018	MZ711319	-	-	-
Galapagomystides patricki n. sp.	SIO-BIC A9961	Jaco Scar, Costa Rica	9.1178° N 84.8395° W	~1785	AD4989	Nov. 4, 2018	MZ711321	-	-	-
Galapagomystides patricki n. sp.	SIO-BIC A9934	Jaco Scar, Costa Rica	9.1175° N 84.8406° W	~1780	AD4989	Nov. 4, 2018	-	-	-	-
Galapagomystides patricki n. sp.	SIO-BIC A1424	cold seep off Costa Rica	9.2123° N84.6425° W	-	G354, MC17	March 4, 2009	-	-	-	-
Galapagomystides aristata	SIO-BIC A12104	NW of Easter Is.. Southern end of the East Pacific Rise	23.8233° S 115.4558° W	~2649	AD4097	April 2, 2005	MZ711263	MZ773006	MZ769000	MZ773065
Galapagomystides aristata	SAM:17169-AD4097 (A-J)	NW of Easter Is.. Southern end of the East Pacific Rise	23.8233° S 115.4558° W	~2649	AD4097	April 2, 2005	MZ711268-MZ711277	-	-	-
Galapagomystides aristata	SAM:17169-SIO-BIC 4092AGala	Saguaro Field, southern EPR, active hydrothermal vents of the Pacific Antarctic Ridge	31.8631° S 112.0422° W	~2334	AD4092	March 27, 2005	MZ711266	-	-	-
Galapagomystides aristata	SAM:17169-SIO-BIC 4092BGala	Saguaro Field, southern EPR, active hydrothermal vents of the Pacific Antarctic Ridge	31.8631° S 112.0422° W	~2335	AD4092	March 27, 2005	MZ711267	-	-	-
Galapagomystides aristata	SAM:17169-SIO-BIC 4091A2Gala	N. German Flats, 38S South East Pacific Rise	37.6725° S 110.877° W	~2236	AD4091	March 25, 2005	MZ711265	-	-	-
Galapagomystides aristata	SAM:17169-SIO-BIC 4091A1Gala	N. German Flats, 38S South East Pacific Rise	37.6725° S 110.877° W	~2236	AD4091	March 25, 2005	MZ711264	-	-	-
Galapagomystides verenae	SIO-BIC A1496A	Mound 12, Costa Rica	8.9285° N 84.3132° W	~1000	AD4502	Feb. 23, 2009	MZ711278	-	-	-
Galapagomystides verenae	SIO-BIC A1496B	Mound 12, Costa Rica	8.9285° N 84.3132° W	~1000	AD4502	Feb. 23, 2009	MZ711279	-	-	-
Galapagomystides verenae	SIO-BIC A1830(A-D)	Jaco Scar, Costa Rica	9.1176° N 84.8395° W	~1800	AD4590	Jan. 11, 2010	MZ711282-MZ711285	-	-	-
Galapagomystides verenae	SIO-BIC A1918	Mound 12, Yettisburg, Costa Rica	8.9308° N 84.3125° W	~995	AD4588	Jan. 9, 2010	MZ711308	-	-	-
Galapagomystides verenae	SIO-BIC A3263 (A-E)	Pinkie's "Vent" North, Guaymas Basin, Gulf of California	27.5969° N 111.487° W	~1580	D380	April 10, 2012	MZ711309-MZ711313	-	-	-
Galapagomystides verenae	SIO-BIC A1477A	Mound 12, Costa Rica	8.93° N 84.3135° W	~1000	AD4501	Feb. 22, 2009	MZ711286	-	-	-
Galapagomystides verenae	SIO-BIC A1312	Mound 12, Costa Rica	8.93° N 84.3135° W	~1000	AD4501	Feb. 22, 2009	MZ711289	-	-	-
Galapagomystides verenae	SIO-BIC A1331	Mound 12, Costa Rica	8.9285° N 84.3132° W	~1000	AD4502	Feb. 23, 2009	-	-	-	-
Galapagomystides verenae	SIO-BIC A8359	Jaco Scar, Costa Rica	9.1156° N 84.8401° W	~1850	AD4913	May 28, 2017	MZ711288	-	-	-
Galapagomystides verenae	SIO-BIC A8379	Jaco Scar, Costa Rica	9.1175° N 84.8395° W	~1750	AD4914	May 29, 2017	MZ711287	-	-	-
Galapagomystides verenae	SIO-BIC A8466	Parrita Seep, Costa Rica	9.0305° N 84.6202° W	~1400	AD4924	June 7, 2017	MZ711290	-	-	-
Galapagomystides verenae	SIO-BIC A8353	Parrita Seep, Costa Rica	9.1154° N 84.8362° W	~1800	AD4912	May 27, 2017	MZ711280	-	-	-
Galapagomystides verenae	SIO-BIC A7991(A-M)	Axial Seamount (CASM), Juan de Fuca Ridge	45.9892° N 130.0267° W	~1550	D876	Aug. 1, 2016	MZ711291-MZ711303	MZ773007	MZ769001	MZ773066
Galapagomystides verenae	SIO-BIC A8563(A-D)	Active rocks above Jackson's hole, Guaymas Basin	27.5893° N 111.4716° W	~1690	D389	April 15, 2012	MZ711304-MZ711307	-	-	-
Galapagomystides verenae	SIO-BIC A10044	Jaco Scar, Costa Rica	9.1174° N 84.8396° W	~1814	S0212 Q9	Jan. 6, 2019	MZ711281	-	-	-

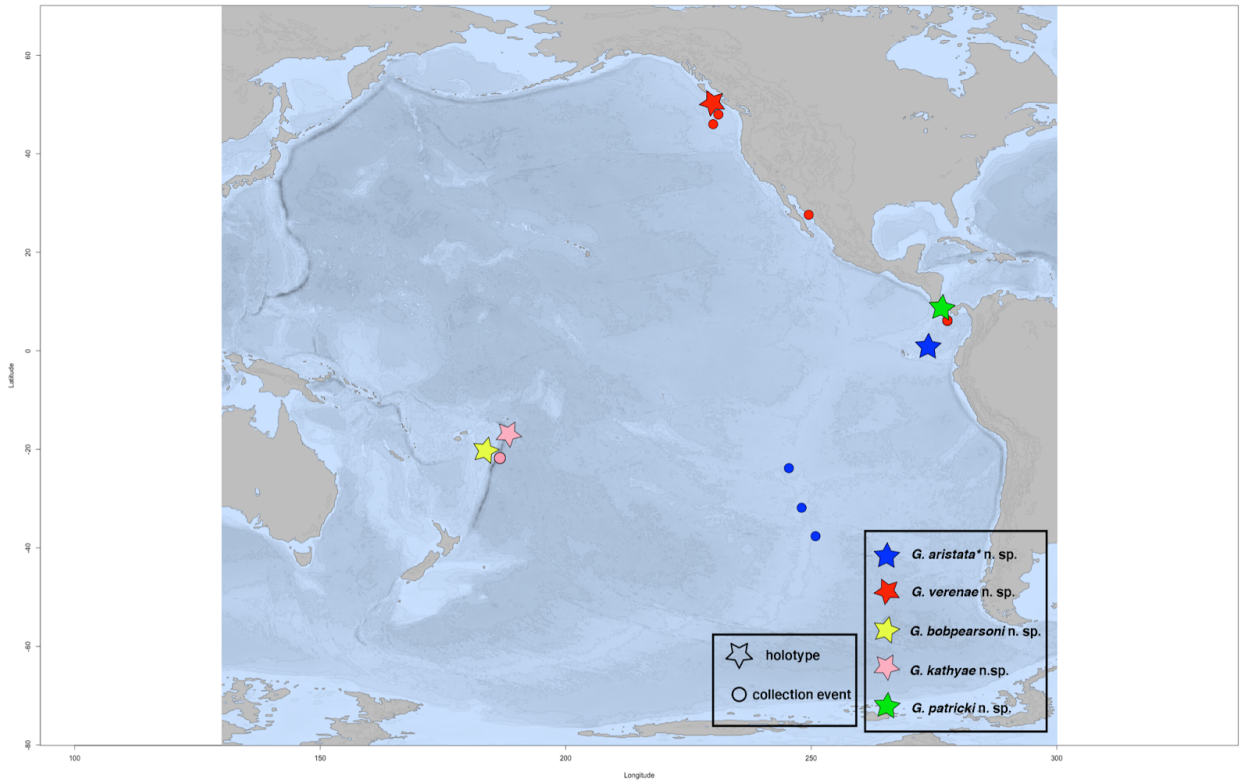

Figure 1. Geographic distribution of *Galapagomystides* species in the Pacific Ocean. *Galapagomystides aristata* was not collected from its type locality, while all other taxa were.

Holotypes and paratypes of the three new species and additional material of *G. aristata* and *P. verenae* are deposited at the Benthic Invertebrate Collection at Scripps Institution of Oceanography (SIO-BIC), UC San Diego in La Jolla, California, USA. Additional material of *G. aristata* is deposited at the South Australian Museum, Adelaide, Australia. Paratypes of *G. aristata* and *P. verenae* were borrowed from the Natural Museum of National History (NMNH), Smithsonian Institution for morphological study; a single specimen for each species was integrated into the SIO-BIC collection (*G. aristata* NMNH 081794= SIO-BIC A13574; *G. verenae* NMNH 122686= SIO-BIC A13575).

Morphological Analysis

Specimens were examined using stereo microscopy (Leica S8 APO and/or Leica MZ9.5), compound light microscopy (Leica DMR HC with differential interference contrast) and scanning electron microscopy (SEM), using a Zeiss EVO 10. Parapodia were mounted on slides permanently using 'Aquamount'® [Thermo Fisher Scientific]. Light micrographs were taken with a Canon EOS Rebel T6i camera. For SEM preparation, specimens were dehydrated in an ethanol series, transferred to Hexamethyldisilazane (HMDS), and then air dried. Dried specimens were then mounted on aluminum stubs employing double-sided carbon adhesive tabs and tape, and sputter-coated with gold-palladium (Au-Pd).

DNA Extraction, Amplification, and Sequencing

DNA was extracted from specimens preserved and fixed in 95% ethanol with the Zymo Research DNA-Tissue Miniprep or Microprep kits using the manufacturer's protocol. DNA sequences for mitochondrial cytochrome c oxidase subunit I (COI), 16S rRNA (16S), nuclear 18S rRNA (18S) and 28S rRNA (28S) were amplified using primers as shown in Table 2. PCR amplification was carried out with 12.5 µl Apex 2.0x Taq Red DNA Polymerase Master Mix (Genesee Scientific), 1µl each of the appropriate forward and reverse primers (10µM, 8.5µl ddH_2O, and 2µl eluted DNA and Eppendorf thermal cyclers. Up to 658 base pairs were amplified for COI with a temperature reaction profile as follows: Initial denaturation at 95°C (3 minutes), followed by 40 cycles of denaturation at 95°C (40 seconds), annealing at 42°C (45 seconds), elongation at 72°C (50 seconds), and final extension at 72°C (5 minutes). Up to 506 base pairs were amplified for 16S with a temperature reaction profile as follows: Initial denaturation at 95°C (3 minutes), followed by 35 cycles of denaturation at 95°C (40 seconds), annealing at 50°C (40 seconds), elongation at 72°C (50 seconds), and final extension at 72°C (5

minutes). Up to 1870 base pairs were amplified for 18S with a temperature reaction profile as follows: 18S-1F and 18S-5R, 18S-a2.0 and 18S-9R: Initial denaturation at 95°C (3 minutes), followed by 40 cycles of denaturation at 95°C (30 seconds), annealing at 50°C (30 seconds), elongation at 72°C (90 seconds), and final extension at 72°C (8 minutes); 18S-3F and 18S-bi: Initial denaturation at 95°C (3 minutes), followed by 40 cycles of denaturation at 95°C (30 seconds), annealing at 52°C (30 seconds), elongation at 72°C (90 seconds), and final extension at 72°C (8 minutes). Up to 1650 base pairs were amplified for 28S with a temperature reaction profile as follows: 28SC1 and 28S1100: Initial denaturation at 95°C (3 minutes), followed by 40 cycles of denaturation at 95°C (40 seconds), annealing at 48°C (45 seconds), elongation at 72°C (50 seconds), and final extension at 72°C (5 minutes); 28S900 and 28S1900: Initial denaturation at 94°C (3 minutes), followed by 35 cycles of denaturation at 94°C (45 seconds), annealing at 52°C (45 seconds), elongation at 72°C (60 seconds), and final extension at 72°C (8 minutes). PCR products were purified using ExoSAP-IT with the manufacturer's protocol (USB, Affymetrix, Ohio). Sanger sequencing was performed by Eurofins Genomics (Louisville, KY). Consensus sequences were assembled using the "De Novo Assembly" option on Geneious v.11.0.5 (Kearse *et al*. 2012) under default settings. All sequences generated for this study were deposited into GenBank (Table 2).

Table 2. Primers used for each specified gene, with references.

Gene	Primer Name & Direction	Primer Sequence (5'-3' Direction)	Source
COI	polyLCO (F)	(5'-GAYTATWTTCAACAAATCATAAAGATATTGG-3')	(Carr et al. 2011)
COI	polyHCO (R)	(5'-TAMACTTCWGGGTGACCAAARAA TCA-3')	(Carr et al. 2011)
16S	16SarL (F)	(5'-CGCCGTTTATCAA AAACAT-3')	(Palumbi et al. 1991)
16S	16SbrH (R)	(5'-CCGGTCTGAACTCAGATCACGT-3')	(Palumbi et al. 1991)
28S	28SC1 (F)	(5'-ACCCGCTGAATTTAAGCAT-3')	(Lê et al., 1993)
28S	28S1100 (R)	(5'-AGGCATAGTTCACCATCTTTCG-3')	(San Martin et al. 2020)
28S	28S900 (F)	(5'-CCGTCTTGAAACACGGACCAAG-3')	(Lockyer et al., 2003)
28S	28S1900 (R)	(5'-CCATGTTCAACTGCTGTTCACATG-3')	(San Martin et al. 2020)
18S	18S-1F (F)	(5'-TACCTGGTTGATCCTGCCAGTAG-3')	(Giribet et al. 1996)
18S	18S-5R (R)	(5'-CTTGGCAAATGCTTTCGC-3')	(Giribet et al. 1996)
18S	18S-3F (F)	(5'-GTTCGATTCCGGAGAGGGA-3')	(Giribet et al. 1996)
18S	18S-bi (R)	(5'- GAGTCTCGTTCGTTATCGGA-3')	(Whiting et al. 1997)
18S	18S-a2.0 (F)	(5'- ATGGTTGCAAAGCTGAAAC-3')	(Whiting et al. 1997)
18S	18S-9R (R)	(5'- GATCCTTCCGCAGGTTCACCTAC-3')	(Giribet et al. 1996)

Phylogenetic Analyses

New sequence data from this study, along with data for *Endovermis seisuiae* Jimi, Kimura, Ogawa and Kajihara 2020 (Jimi *et al.* 2020) were added to the data set sourced from San Martín *et al.* (2020). The tree was rooted with *Lumbrinereis latreilli* Audouin & Edwards 1833, and other non-Phyllodocidae terminals following San Martín *et al.* (2020). We excluded the COI data for *Lumbrinereis latreilli*, *Glycera dibranchiata* and *Paralacydonia paradoxa* listed by San Martín *et al.* (2020) because these were from the wrong region of COI. Sequences were aligned with MAFFT 7 using the Q-INS-I setting (Katoh and Standley 2013). Aligned sequences for genes COI, 16S, 18S and 28S were concatenated with Sequence Matrix Vaidya *et al.* 2011). A maximum likelihood (ML) analysis was conducted with RAxML-NG (Kozlov 2019) using RAxML GUI v.2.0 (Edler *et al.* 2021). Bayesian Inference (BI) was also performed using MrBayes 3.2.7 (Ronquist *et al.* 2012). Sequences were partitioned by gene, and the following optimized models were chosen using ModelTest-NG (Darriba *et al*. 2020); 16s: HKY+I+G. 18s: TIM1+I+G.

28s: TIM3+I+G. COI: GTR+I+G. Node support for ML was assessed via thorough bootstrapping (with 1,000 pseudoreplicates).

Uncorrected pairwise distances for COI sequences among the five species studied here were generated with Geneious v.11.0.5. (Table 3). Sequences of the holotypes were used for the three new species. Sequence data from the type locality were used for *G. verenae that had* the minimum distance to any other species and this was also done for the *G. aristata* sequences from the EPR. Haplotype networks using COI data were generated with PopART v.1.7 (Leigh and Bryant 2015) for *G. patricki* n. sp., *G. aristata* and *G. verenae* using the median-joining option (Bandelt *et al.* 1999). Habitat (Seep or Vent) and biogeography (East or West Pacific) transformations were generated with Mesquite v.3.61 (Maddison and Maddison 2019) using the most parsimonious transformations and maximum likelihood transformations under the Mk1 model (Lewis 2001).

Results

Phylogeny and species delimitation

The ML and BI analyses of the concatenated molecular data were congruent (Fig. 2, outgroups excluded) and matched the results of San Martín *et al*. (2021) with respect to the data they provided. The full phylogenetic results including outgroups is shown in Figure 21. Phyllodocidae fell into two major clades of similar size, marked here as A and B, though neither was well supported. *Galapagomystides aristata* and the three new species formed a well-supported clade in Clade A along with *Protomystides verenae,* which was sister group to *G. kathyae* n. sp. For this reason *Protomystides verenae* is referred *to* as *Galapagomystides verenae*. The sister group to the *Galapagomystides* clade was *Pterocirrus nidarosiensis*, though

with low support. *Galapagomystides patricki* n. sp. was the sister taxon to a well-supported clade comprising the remaining *Galapagomystides* species. *Galapagomystides bobpearsoni* n. sp. and *G. aristata* formed a grade with respect to the *G. kathyae* n. sp. and *G. verenae* clade. The only other new terminal added to the dataset used in San Martín *et al*. (2021) was *Endovermis seisuiae* and this formed a clade with *Paranatis* spp. (Fig. 2).

Uncorrected pairwise distances for the COI sequences (Table 3) showed distances among the five *Galapagomystides* species ranging from 13.1% to 19.7%.

Table 3. Minimum uncorrected pairwise distances for COI among the five species of *Galapagomystides*.

	G. aristata	*G. verenae*	*G. bobpearsoni* n. sp.	*G. kathyae* n. sp.	*G. patricki* n. sp.
G. aristata	-				
G. verenae	13.1%	-			
G. bobpearsoni n. sp.	14.8%	17.3%	-		
G. kathyae n. sp.	13.1%	14.5%	16.1%	-	
G. patricki n. sp.	17.2%	19.7%	17.8%	17.6%	-

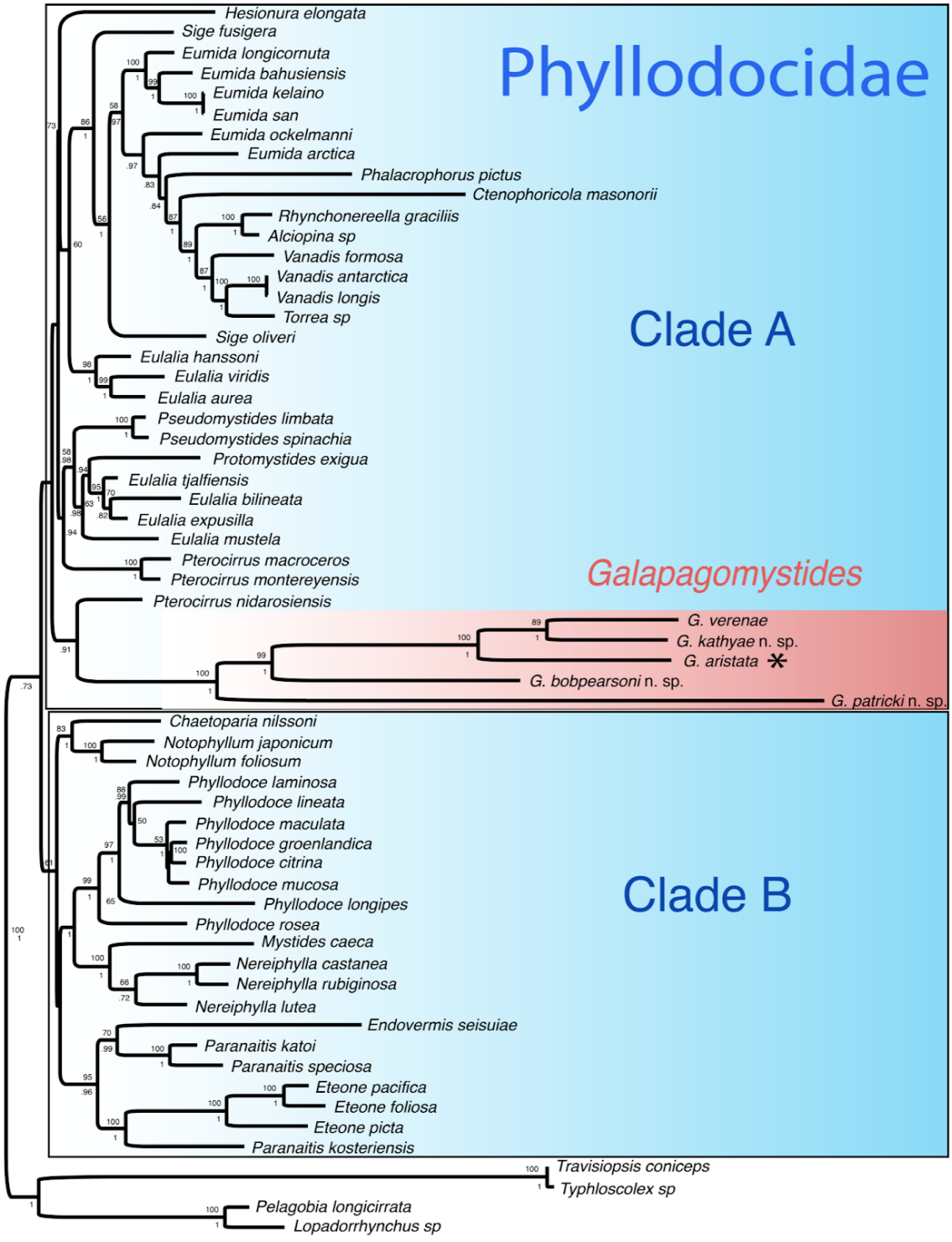

Figure 2. Maximum Likelihood (ML) tree generated from the concatenation of genes COI, 18S, 28S and 16S. Numbers on nodes represent ML bootstrap values (above node) and Bayesian posterior probabilities (below node). Values below 50% for ML and 0.70 for posterior probabilities are not shown. '*' indicates type species.

Haplotype Networks

Twelve specimens of *G. aristata* from 1,500 km along the East Pacific Rise were included in the COI haplotype network (Fig. 3), which displayed three distinct haplotypes, varying maximally by two base pair differences. One haplotype was dominant and occurred in all three sampled locations.

Galapagomystides verenae specimens were collected from hydrothermal vents off Oregon, near the type locality, as well as methane seeps off Costa Rica, and the Guaymas Basin (Mexico). The 38 specimens included in the COI haplotype network (Fig. 4) showed 17 different haplotypes over a geographic range of ~6500 km. The maximum intraspecific uncorrected pairwise distance represented across this network was 1.4%. Two haplotypes were found that spanned this entire range. This network shows that *G. verenae* is not depth restricted with two haplotypes being found across nearly 1000 m. of depth difference.

The 8 specimens of *G. patricki* n. sp. included in the COI haplotype network displayed six haplotypes (Fig. 5). These were collected from two localities off Costa Rica that differed in depth by 400 m. The maximum intraspecific uncorrected pairwise distance represented across this network was 2.1%, all from samples at the same site, Parrita Seep, Costa Rica.

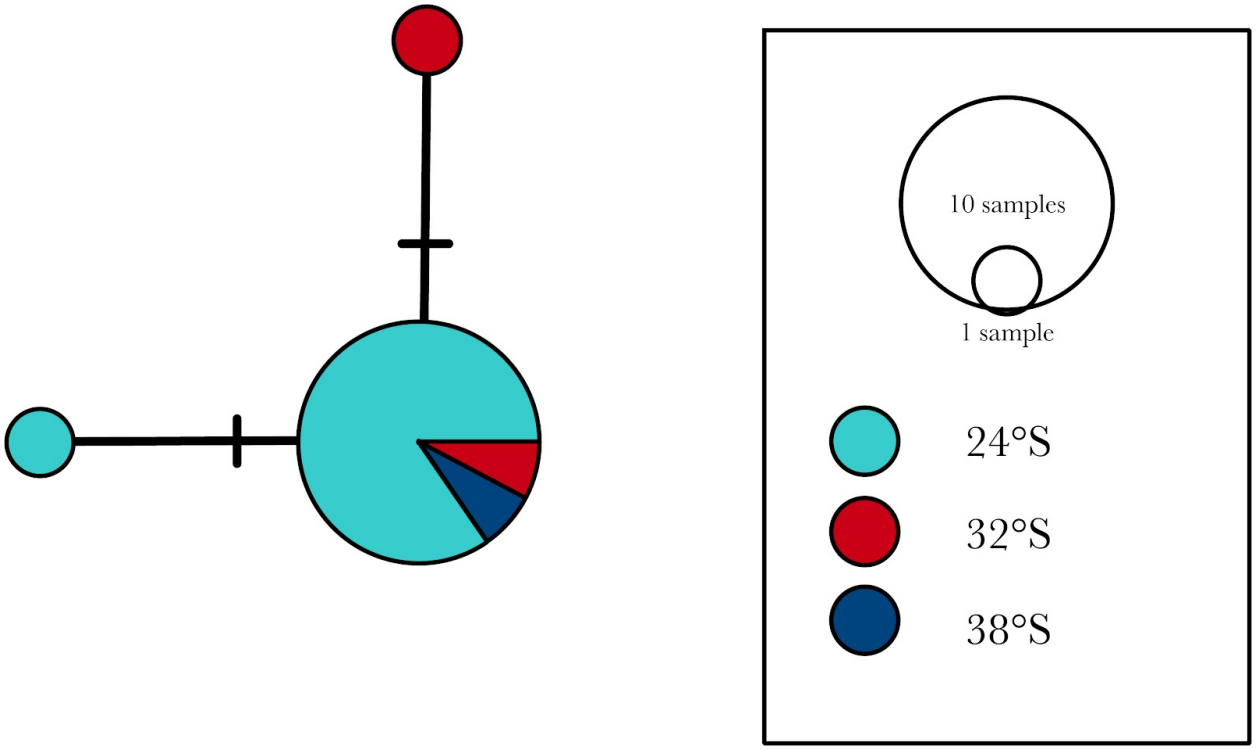

Figure 3. *Galapagomystides aristata* haplotype network. Specimens were collected from over 1,500 km along the East Pacific Rise.

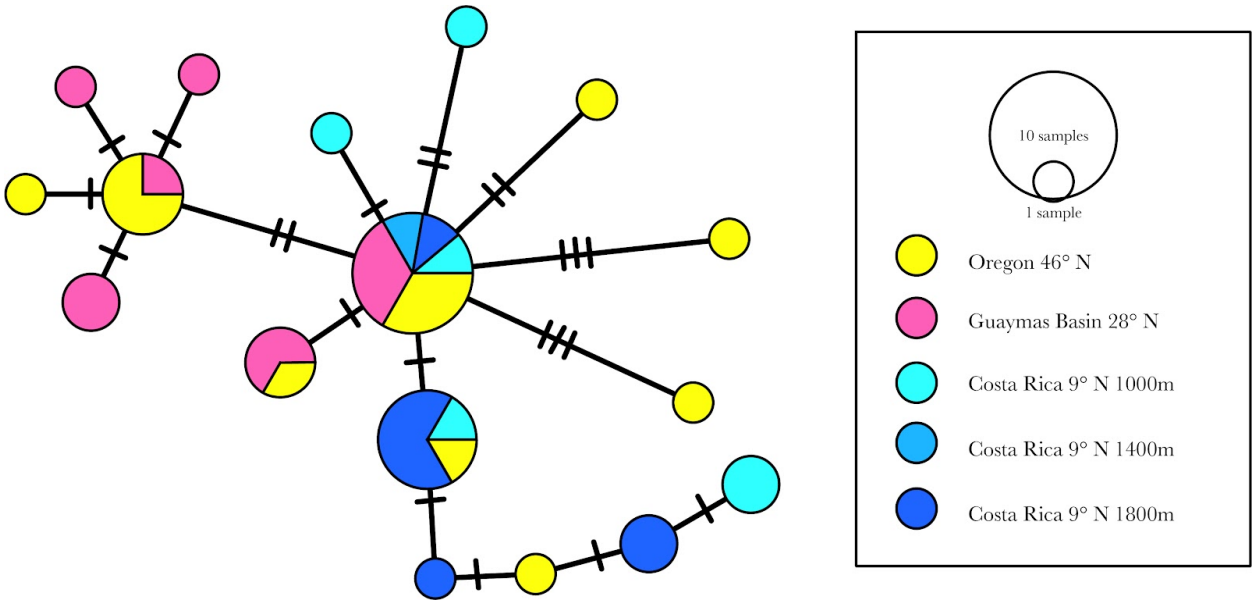

Figure 4. *Galapagomystides verenae* haplotype network. Specimens collected from Costa Rica were sorted into three shades of blue based on varying depth. Oregon is the type locality.

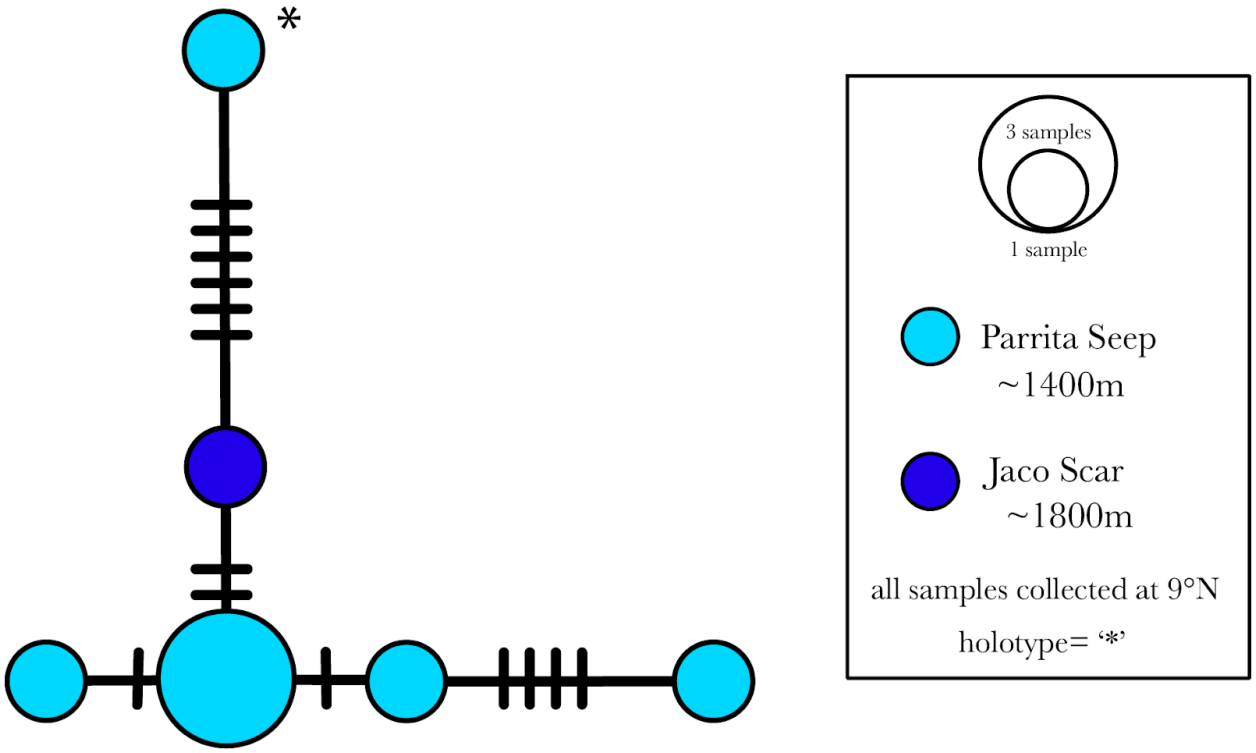

Figure 5. *Galapagomystides patricki* n. sp. haplotype network. All specimens were collected from Costa Rica at two depths.

Habitat Evolution

The most parsimonious reconstruction for habitat evolution (Fig. 6), shows that the ancestral habitat for *Galapagomystides* could have been either event or seep. *Galapagomystides verenae* is the only species found to occupy both vents and seeps. Given its phylogenetic placement nested among the seep-dwelling *Galapagomystide*s, the vent-dwelling populations of *G. verenae* would appear to have colonized from a seep habitat.

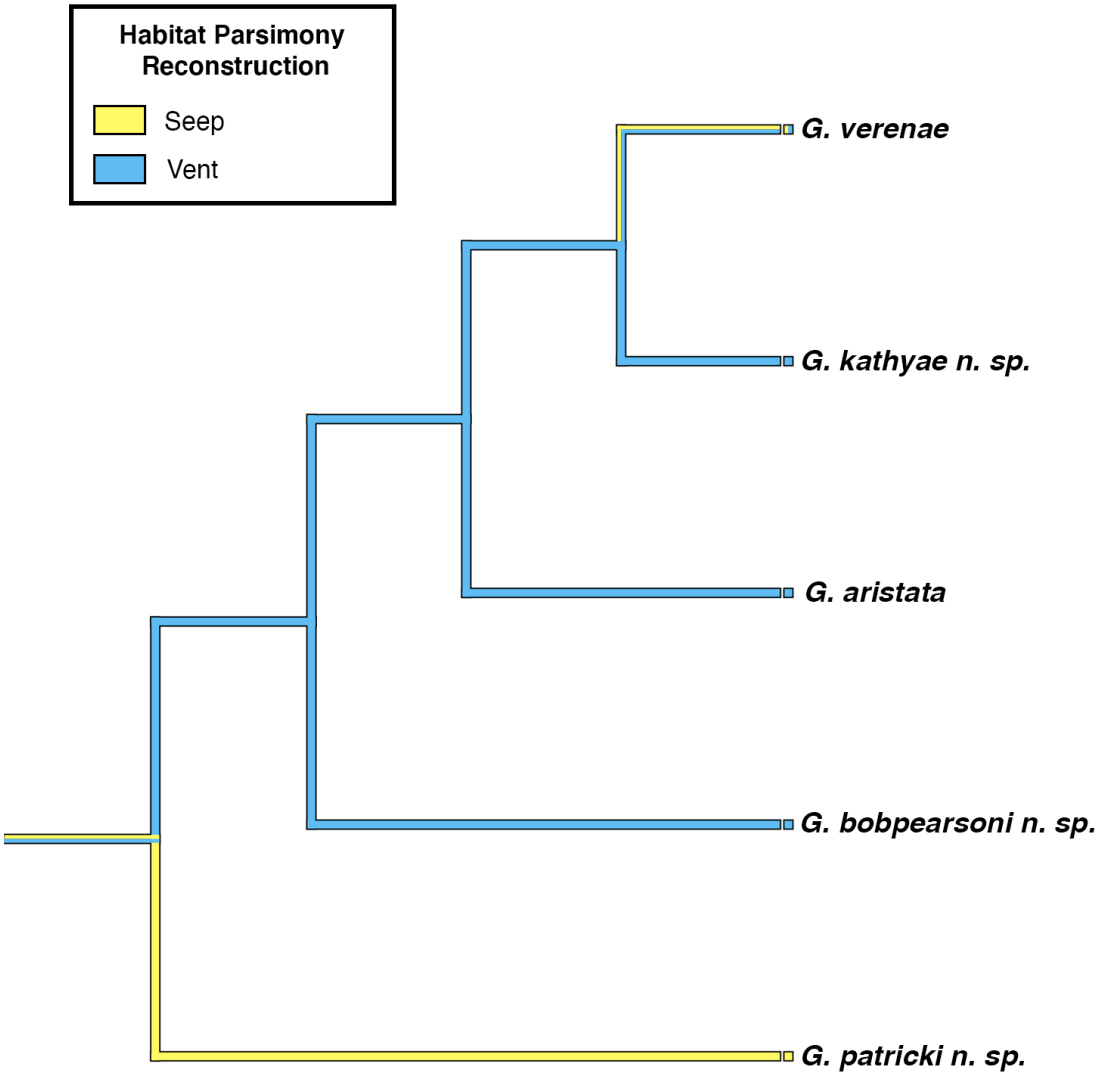

Figure 6. Habitat parsimony reconstruction analysis.

Biogeography

The most parsimonious reconstruction for the geographical distribution of Galapagomystides (Fig. 7) indicates an eastern Pacific origin for the group. There appear to have been two separate colonizations to the western Pacific vents, by *G. kathyae* n. sp. and *G. bobpearsoni* n. sp. respectively.

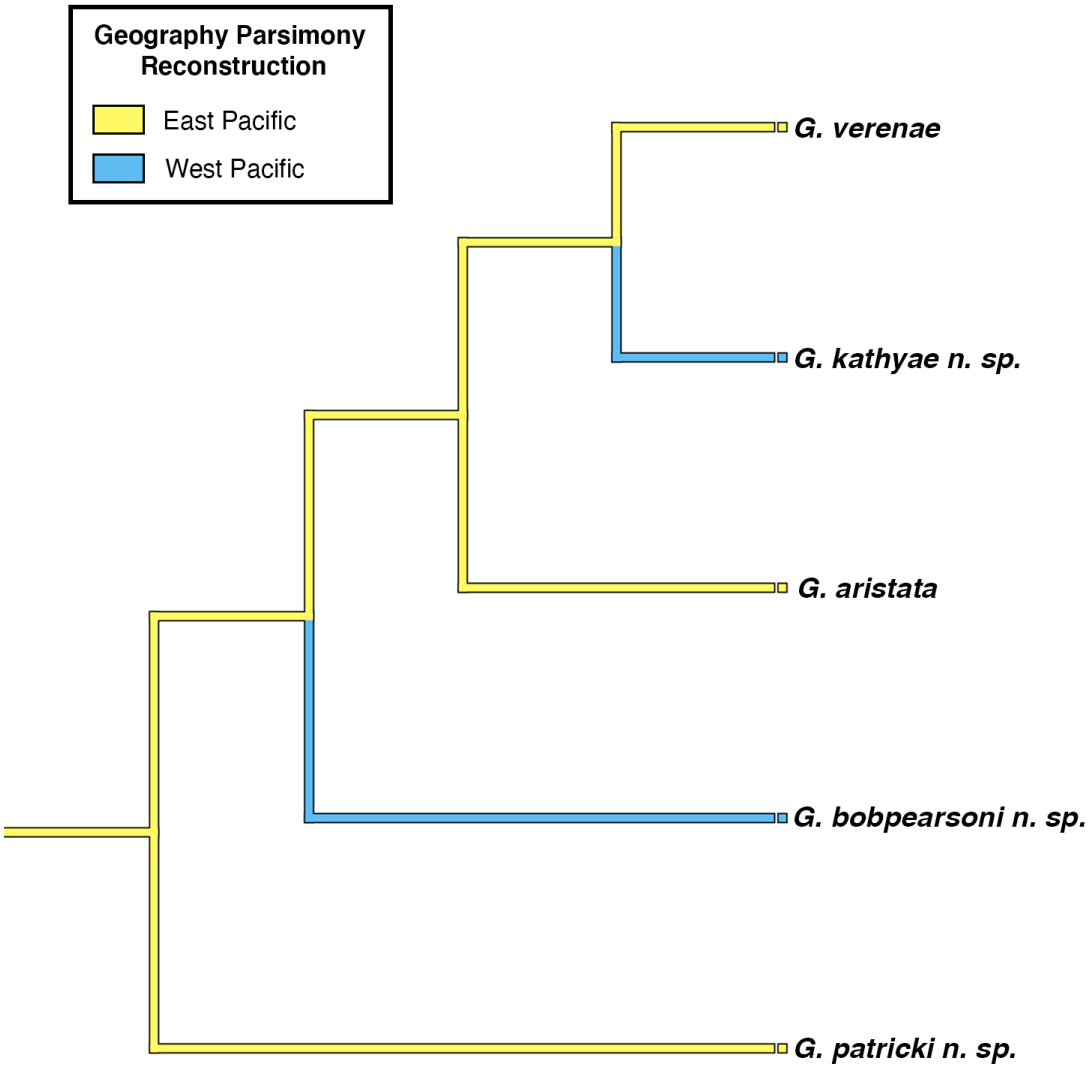

Figure 7. Geography parsimony reconstruction analysis. Yellow represents the East Pacific while blue represents the West Pacific.

Discussion

This is the first study examining the phylogeny, biogeography, and diversity of *Galapagomystides*. By incorporating the new data with those from previous molecular phylogenies of Phyllodocidae (Eklöf *et al*. 2007; San Martin *et al.* 2020) it was possible to assess Pleijel's (1991) hypothesis as to the placement of *Galapagomystides*. Pleijel (1991) proposed that *Galapagomystides* formed the sister group to a clade comprising *Eteone, Hypereteone* and *Mysta.* These taxa along with others such as *Eulalia, Eumida, Protomystides, Pseudomystides, Pterocirrus*, and *Sige* formed the subfamily Eteoninae. The remaining Phyllodocidae were placed in Phyllodocinae (*Chaetoparia*, *Paranaitis* and *Phyllodoce*), and Notophyllinae (*Notophyllum*, *Nereiphylla*). Previously, in his original description of *Galapagomystides aristata*, Blake (1985) suggested that it was closely related to *Mystides*. Figure 2 shows that Pleijel's (1991) tree topology and classification are not supported, with the type species of each subfamily all placed in clade B. *Galapagomystides* was recovered as the poorly-supported sister group to *Pterocirrus nidarosiensis* and is part of clade A, quite distant from *Eteone*. *Mystides* was also found as part of clade A and distant from *Galapagomystides* in clade B. The morphological similarities for grouping *Galapagomystides* as proposed by Blake (1985) and Pleijel (1991) do not seem to be supported. However, clades A and B were both poorly supported (Fig. 2) and more data are needed to resolve the phylogeny of Phyllodocidae and allow for a taxonomic revision of the group. The long branch shown by the *Galapagomystides* clade may also indicate that its position shown in Figure 2 may not be accurate. As well as documenting three new species, the results show that another vent-dwelling member of Phyllodocidae, *Protomystides verenae*, should be transferred to *Galapagomystides*. A revised morphological diagnosis for *Galapagomystides* is below in the **Taxonomy** section.

The biogeographical analysis (Fig. 7) indicates that there are two near sympatric species of *Galapagomystides* at western Pacific vents, and three species in the eastern Pacific, two of which are sympatric at Costa Rican seeps. The western Pacific species, *G. bobpearsoni* n. sp. and *G. kathyae* n. sp., are not each other's closest relatives, suggesting they independently colonized these sites. Also, *G. verenae* and *G. patricki* n. sp. were found in close proximity off Costa Rica at Parrita Seep and are not closely related. This phenomenon has been observed in other annelid taxa including *Amphisamytha* (Stiller *et al.* 2013) and *Archinome* (Borda *et al*. 2013) and *Parougia* (Yen and Rouse, 2020). *Galapagomystides verenae* has a very wide distribution at both vents and seeps and may have colonised the Costa Rican seeps, as it appears to have a vent ancestry (Fig. 6). It is not common to find a species living at both vents and seeps (Kiel, 2016; Sibuet and Olu, 1998; Wolff, 2005; Watanabe *et al*. 2010; Tunnicliffe *et al*. 1998, 2003; Peek *et al*. 1997) as seen in vent-endemic *Bathykurila guaymasensis* Pettibone 1989 (Smith and Baco, 1998) and vestimentiferan tubeworm genera *Riftia*, *Oasisia*, *Ridgeia* and *Tevnia* (Black *et al*. 1997). However, within Annelida, the ampharetid *Amphisamytha fauchaldi* lives at vents in the Gulf of California and seeps from Oregon to Costa Rica and the amphinomid *Archinome levinae* also lives at vents in the Gulf of California and seeps off Costa Rica (Stiller *et al*. 2013; Borda *et al*. 2013).

Protomystides hatsushimaensis has been recorded from seeps and vents in the northwestern Pacific and associated with Vestimentifera (Kobayashi and Kojima 2017). This species also may prove to be a member of *Galapagomystides* once DNA sequence data is made available. The record of a blood-feeding *'Protomystides'* in the Gulf of Mexico (Becker *et al.* 2013) that has also not been described, let alone sequenced, suggests that further *Galapagomystides* species will be discovered and so the present phylogenetic hypothesis is incomplete.

The type locality of *G. verenae* is the Juan de Fuca hydrothermal vent systems along the Cascadia Subduction Zone (CSZ) of the northeastern Pacific Ocean, though from evidence provided here, the species also extends much further south at methane seeps. The type locality of *G. aristata* is at the Galapagos Rift vents and it would appear from this and other studies (Jenkins *et al.* 2002; Govenar *et al.* 2004) that it occurs along the East Pacific Rise. These disjunct vent systems were once connected as part of the Pacific-Farallon Ridge, which was disrupted by subduction under the North America plate nearly 30 million years ago (mya) (Chevaldonné *et al.* 2002). Chevaldonné *et al*. (2002) proposed to use this vicariant event as a way of calibrating molecular clocks and assessed this for several proposed annelid sister species pairs that occurred at the northeastern Pacific vents and the EPR. It was later shown that their proposed sister species pairs were not actually sister taxa and so their molecular clock rate has been questioned (Stiller *et al.* 2013), but the use of the calibration point still has merit. The results shown here suggest that *G. aristata* and *G. verenae* are closely related, but are not sister taxa since *G. kathyae* n. sp. was actually recovered as the sister group to *G. verenae* (Fig. 2). It would seem reasonable that the split between the *G. aristata* and the *G. kathyae* n. sp/ *G. verenae* clade could be dated at around 30 mya.

Galapagomystides has been inferred to feed on the blood of Vestimentifera based on anatomical studies (Jenkins *et al.* 2002) and there are numerous ecological studies associating them with Vestimentifera (Becker *et al.* 2013; Govenar *et al.* 2004;Govenar *et al.* 2005;Tsurumi and Tunnicliffe, 2003;Govenar and Fisher 2007). There was a higher *G. aristata* concentration in real *Riftia pachyptila* tube assemblages when compared with the artificial tube assemblages, suggesting that *G. aristata* were there to feed on the real *Riftia pachyptila.* Further photo documentation (Fig. 14) of *Galapagomystides verenae* atop juvenile *Escarpia spicata* tubes is provided here as well as *G. patricki* n. sp. living inside tubes in Vestimentifera tubes (Fig. 19A).

Contrary evidence to a blood diet for *Galapagomystides* has been provided in a stable isotope study (Berqguist *et al.* 2007) that showed *G. verenae* had δ13C and δ15N values suggesting a diet containing the annelid *Nicomache venticola* Blake and Hilbig 1990 and the gastropod *Depressigyra globulus* Warén & Bouchet, 1989. Both of these prey items lack external gills, feeding plumes or blood-accessible features.

Taxonomy

Phyllodocidae Ørsted, 1843

***Galapagomystides* Blake, 1985 (emended)**

(Pleijel 1991; Blake 1994)

Table 4.

Type species. *Galapagomystides aristata* Blake, 1985

Diagnosis (emended). Prostomium wider than long. Two antennae; two palps similar in size/shape to antennae. No median antenna or nuchal papilla. Nuchal organs unknown. Eyes absent. Smooth proboscis, papillae at distal end. Segment 1 fused or not (dorsally) to prostomium. Segment 1 distinct ventrally. Elongated dorsal cirri (EDC) (= tentacular cirri) on segments 1, 2; EDC on segment 3. No ventral cirri on segment 1. Ventral cirri on segment 2 elongated or similar to following segments. Parapodia uniramous, notopodial chaetae absent. Neuropodium with central fascicle containing compound chaetae; one simple emergent acicula. Compound chaetal shaft cylindrical; pointed blade extended from fulcate joint. Rostrum of chaetal shaft asymmetrical/hooked. Presence of segmental bands of cilia. Pygidial cirri robust ellipsoid lobes. Living animals are red.

Remarks. Based on this study, *Galapagomystides* now includes five species; *G. aristata*, *G. bobpearsoni* n. sp, *G. kathyae* n. sp., *G. patricki* n. sp., and *G. verenae*. Blake's

(1985) original *Galapagomystides* diagnosis stated that the genus has segment 1 fused dorsally to the prostomium, and no dorsal cirri on segment 3. We amend the *Galapagomystides* diagnosis to allow for the variation shown in other members of the genus. For instance some taxa do not have segment 1 fused to the prostomium, and may have dorsal elongated cirri on segment 3 in addition to segments 1 and 2 (Table 4). Pleijel's (1991) diagnosis of *Galapagomystides* accepted Blake's (1985) diagnosis, with the addition of nuchal organs present as dorso-lateral ciliated pits between the prostomium and segment 1. Pleijel (1991) also questioned the presence of segmental ciliated bands though their presence is confirmed here. All species within *Galapagomystides* have an asymmetrical/hooked tip of the chaetal shaft, which is unique to the genus among Phyllodocidae. For a morphological summary of variation within *Galapagomystides* see Table 4.

Table 4. Features of *Galapagomystides* species. (1) = present. (0) = absent.

feature presence	**elongated dorsal cirri** segment			**elongated ventral cirri** segment			**segment 1 fusion to prostomium**
	1	2	3	1	2	3	
G. aristata	1	1	0	0	1	0	1
G. verenae	1	1	1	0	1	0	0
G. bobpearsoni n. sp.	1	1	1	0	1	0	1
G. kathyae n. sp.	1	1	1	0	1	0	1
G. patricki n. sp.	1	1	0	0	0	0	0

***Galapagomystides aristata* Blake 1985**

Figures 8-10.

Cordes *et al*. (2007), Becker *et al*. (2013), Blake (1985, 1994), Desbruyères *et al*. (1997, 2006), Dreyer (2004), Gollner *et al*. (2015), Govenar *et al*. (2004, 2005, 2007), Jenkins *et al*. (2002), Rodrigo *et al*. (2015), Scharhauser (2013), Tunnicliffe (1992, 1998), Van Dover (2002), Ward *et al*. (2003)

Diagnosis. *Galapagomystides* with first segment fused dorsally to prostomium. Elongated dorsal cirri on segments 1 and 2. Elongated ventral cirri on segment 2. Exaggerated hook-like joint of compound chaetae.

Material Examined. Paratypes: A13574, Galapagos Rift Geothermal Vents, ~2,500 meters depth; SIO-BIC: A12104*, SAM:17169:4091A1Gala*, SAM:17169:4091A2Gala*, SAM:17169:4092AGala*, SAM:17169:4092BGala*, SAM:17169:4097A-J*, South East Pacific Rise, ~2,200-2,700 meters depth. For locality details see Table 1. * indicates sequenced specimens.

Description. Up to 22mm long, 1mm wide at segment 10 for ~100 segments. Body semi-translucent and white at parapodial lobes, dorsal and ventral cirri, elongated cirri, pygidial cirri, prostomium and pygidium; deep pink/red in longitudinal center in life (Fig. 8A-D). Body brown/orange with numerous dark pigmentation speckles in preserved (formalin/ethanol) state (Fig 8E). Rounded, lobe-like prostomium; no obvious nuchal organs. Anterior dorsal edge of prostomium with paired cylindrical antennae ~0.2mm long (Fig. 9C). Paired palps ventral to antennae, similar in shape and length to antennae (Fig. 9C). Segment one dorsally fused to prostomium, following segments clearly demarcated (Fig. 9A,C,E). Pair of elongated dorsal cirri [tentacular cirri] on each of segments 1 (~0.25mm long), 2 (~0.28mm long) (Fig. 9A,C). All elongated dorsal cirri cirriform, tapering distally. Pair of elongated ventral cirri on segment 2 (~0.2mm long) (Fig. 9A,C). Conical, tapering regular ventral cirri (~0.08mm long) begin on segment 3 continuing posteriorly (Fig. 9C). Bulbous, rounded dorsal cirri (~0.08mm long) begin

on segment 4 continuing posteriorly (Fig. 9A). Dorsal cirri absent on segment 3 (Fig. 9A). Parapodia uniramous, notopodial chaetae absent; neuropodium with central fascicle containing ~5-8 compound chaetae; one simple emergent acicula (Fig. 8F,H & 10B,D,E). Compound chaetal shaft cylindrical; thin, flattened pointed blade extended from curved joint (Fig. 9D & 10B,D,E). Pygidium with one pair of cirriform pygidial cirri tapering distally (~0.2mm long) (Fig. 9B). Proboscis protrudes ¼ body length, smooth until ½ distance distal, then lined with papillae (Fig. 9E).

Variation. There was a very slight variation in animal length and number of segments in comparison to the original description (Blake 1985). The specimens studied here reached ~100 segments and a total length of 22mm (Fig 8E) as opposed to ~90 segments and a total length of 20mm described by Blake (1985).

Remarks. The *G. aristata* samples used in our DNA analyses were collected along the EPR, which is not the type locality (Galapagos Rift). However, the specimens matched Blake's description closely. Previous authors have recorded *G. aristata* specimens from the EPR, though these were not taxonomic studies. (Jenkins *et al.* (2002) and Govenar *et al.* (2004; 2005). It seems appropriate to extend the range of *G. aristata* to the EPR, though confirmation of this does require DNA sequencing of *G. aristata* from the Galapagos Rift vents. Unique features of *G. aristata* shared between specimens used in this study and the paratypes include the hook-like joint of the compound chaetae (Fig. 9D and 10D), fusion of segment one dorsally but not ventrally to the prostomium (Fig. 9A,C, and 10A,C), the prostomium size and shape (Fig. 9A,C, and 10A,C).

Galapagomystides aristata is morphologically most similar to *G. kathyae* n. sp. and *G. bobpearsoni* n. sp in that all have segment 1 dorsally fused to the prostomium. However, in the phylogenetic analyses, *G. aristata* was found to be the sister group to a clade comprising *G.*

kathyae n. sp. and *G. verenae*. *Galapagomystides aristata* has a smooth proboscis as mentioned in previous descriptions (Blake 1985; Pleijel 1991), though there are papillae located at the distal third of the proboscis (Fig. 9E). Pleijel's (1991) diagnosis of *Galapagomystides* with type species *aristata* claimed nuchal organs present as dorso-lateral ciliated pits between the prostomium and segment 1, however nuchal organs were not located in this study.

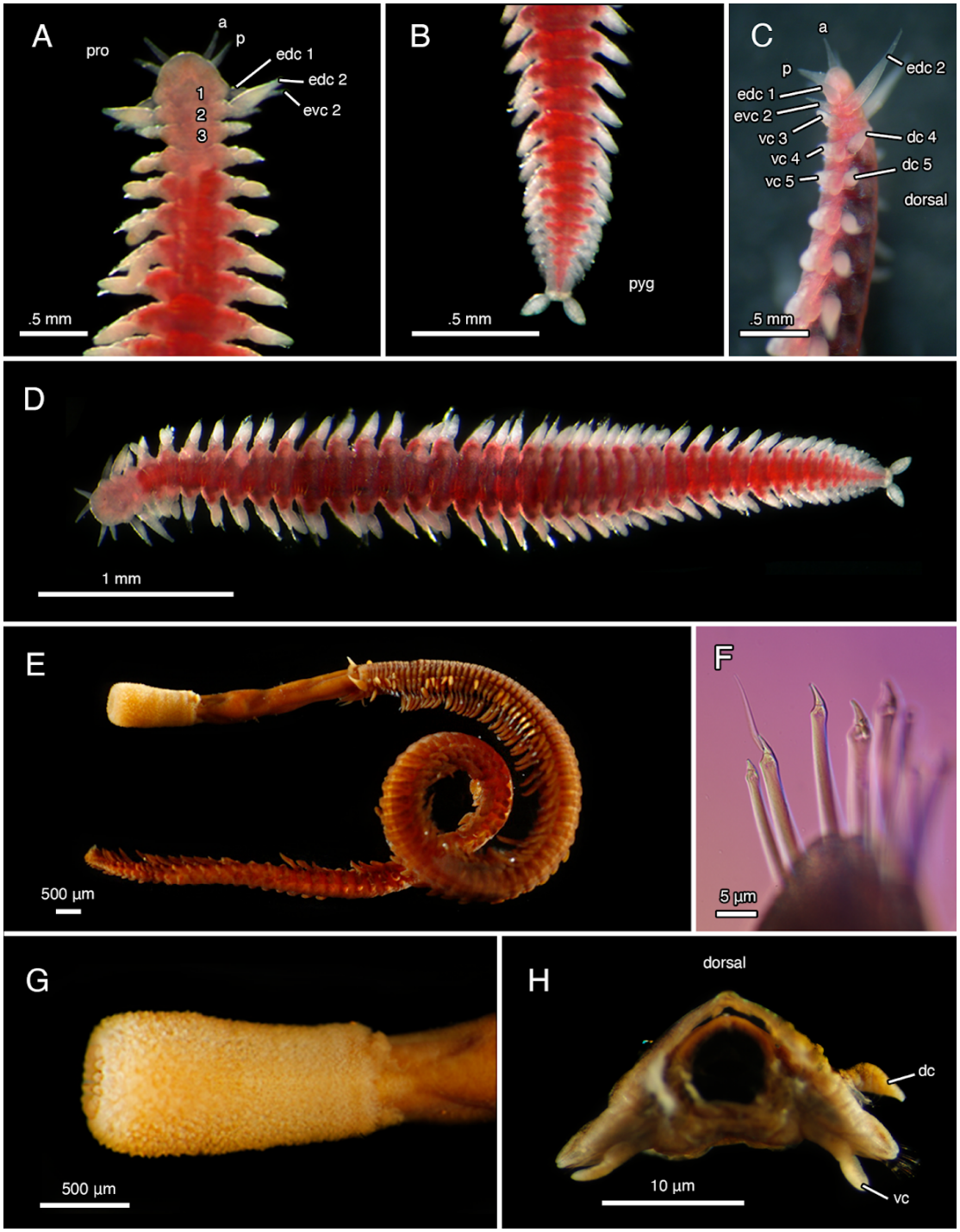

Figure 8. Photos of *Galapagomystides aristata* from the East Pacific Rise. A— dorsal view of anterior, live (SAM:17169 AD4092). B— pygidium, live (SAM:17169 AD4092). C— lateral view of anterior, live (SAM:17169 AD4092). D— dorsal view of whole body, live (SAM:17169 AD4092). E—everted proboscis (SAM:17169 AD4097). F—compound chaetae (SAM:17169 AD4097). G— proboscis (SAM:17169 AD4097). H— parapodia (SAM:17169 AD4097).

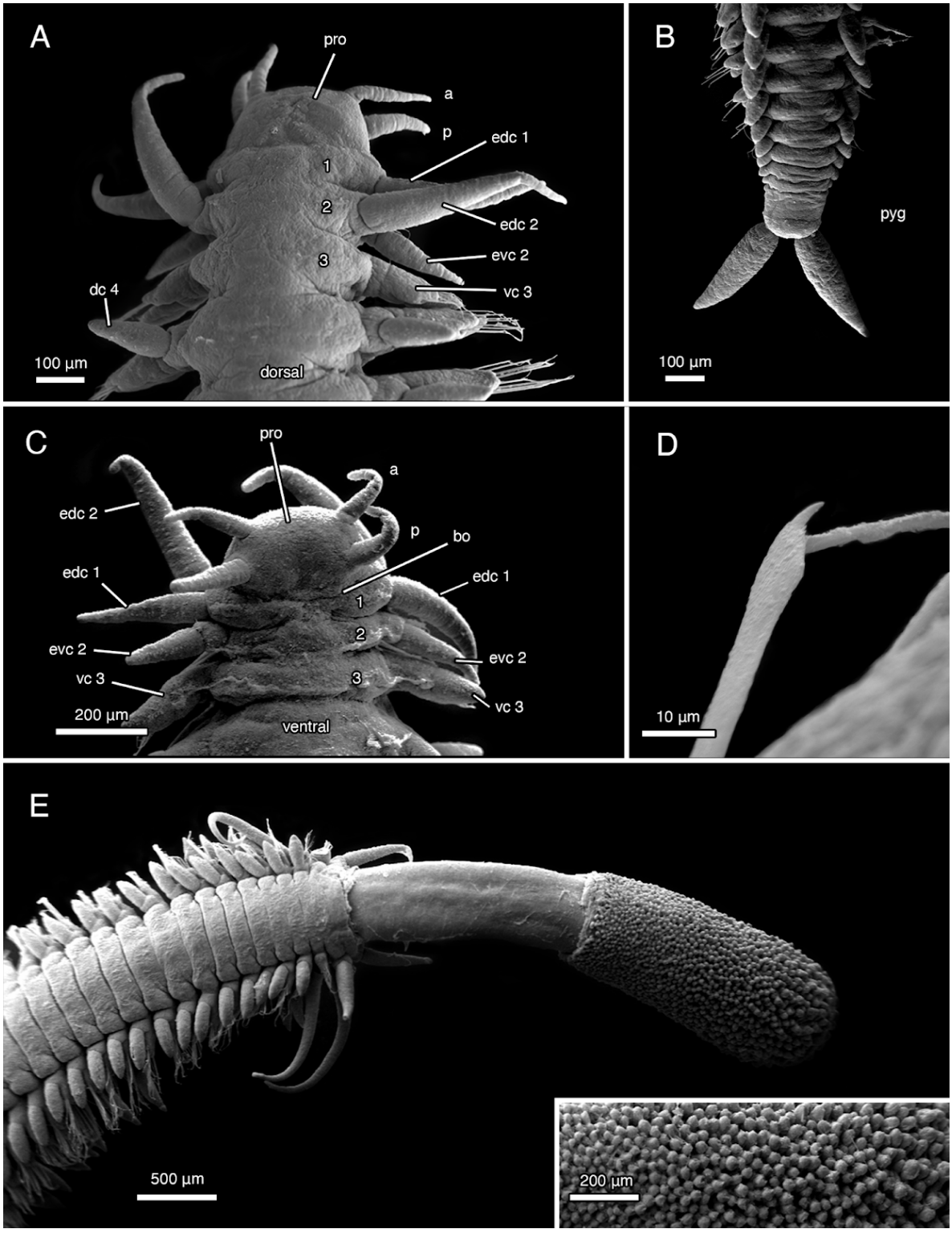

Figure 9. SEM of *Galapagomystides aristata* from the East Pacific Rise. A— dorsal view of anterior (SAM:17169 SIO-BIC AD4092). B— pygidium (SAM:17169 SIO-BIC AD4092). C— ventral view of anterior (SAM:17169 SIO-BIC AD4092). D—zoomed-in compound chaetae joint (SAM:17169 SIO-BIC AD4092). E—everted proboscis, with zoomed-in inlay of papillae (SAM:17169 SIO-BIC AD4097).

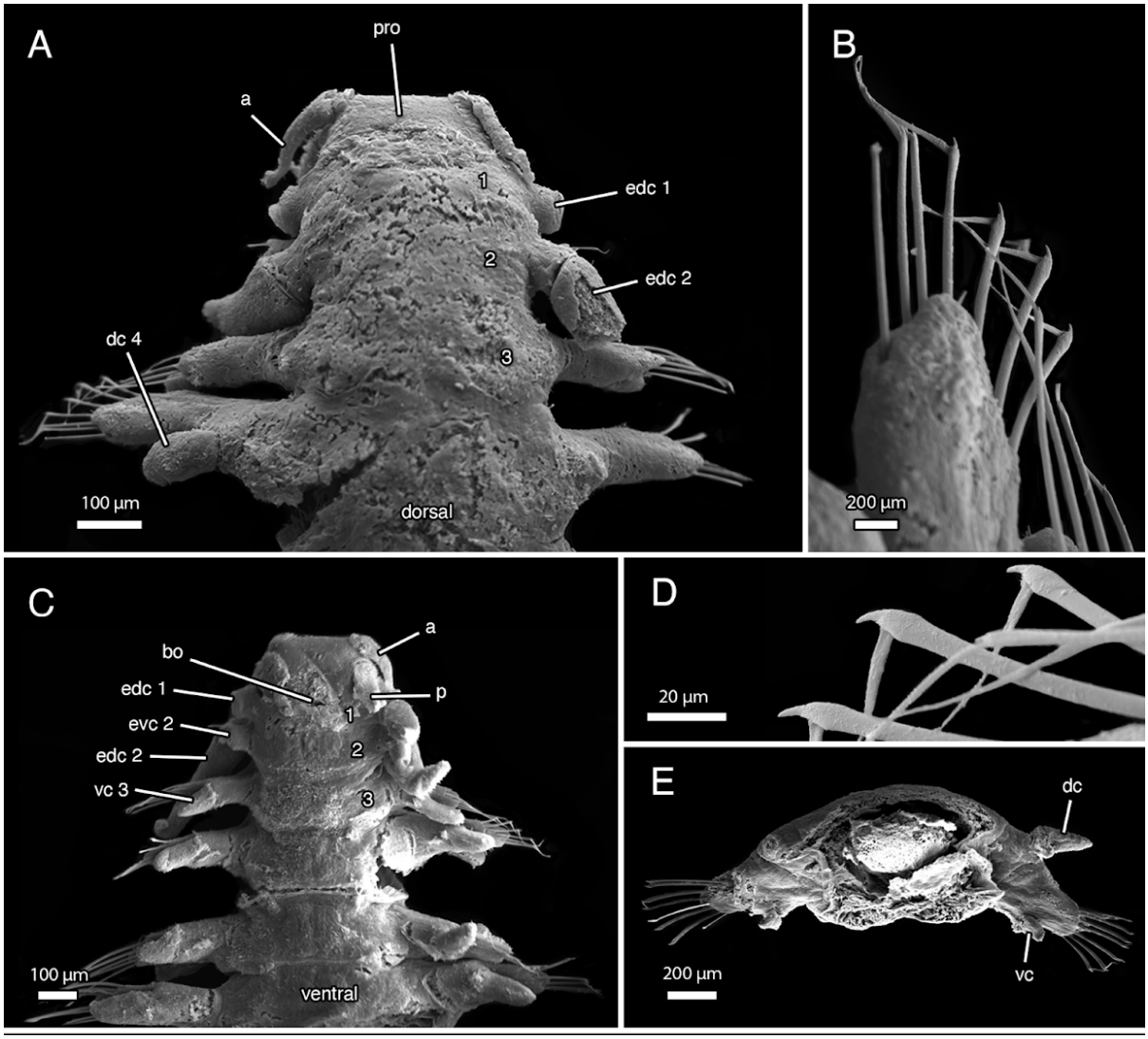

Figure 10. SEM of *Galapagomystides aristata,* paratype voucher (SIO-BIC A13574). A— dorsal view of anterior. B— compound chaetae. C— ventral view of anterior. D—compound chaetae joint. E—parapodia.

Galapagomystides verenae (Blake and Hilbig 1990)

Figures 11-14.

Bergquist *et al*. (2007), Chapman *et al*. (2018), Desbruyères *et al*. (1997, 2006), Kelly *et al*. (2007), Kobayashi and Kojima (2017), Lelièvre *et al*. (2017), Marcus and Anholt (2003), Milligan and Tunnicliffe (1994), Tsurumi and Tunnicliffe (2003), Tunnicliffe (1992), Tunnicliffe *et al*. (1997)

Material Examined. Paratypes: SIO-BIC A13575, Magic Mountain, Explorer Ridge, USA, ~1,810 meters depth; SIO-BIC: A7991(A-M)*, Axial Seamount (CASM), Juan de Fuca Ridge, ~1,550 meters depth; SIO-BIC: A3263(A-E)*, A8563(A-D)*, Guaymas Basin, Mexico, ~1,650 meters depth; SIO-BIC: A1496A*, A1496B*, A1477A*, A1312*, A1331*, A1918*, Mound 12, Costa Rica, 1,000 meters depth; SIO-BIC: A1830(A-D)*, A8359*, A8379*, A10044*, Jaco Scar, Costa Rica, ~1,800 meters depth; SIO-BIC: A8466*, A8353*, Parrita Seep, Costa Rica, ~1,400-1,800 meters depth. For locality details see Table 1. * indicates sequenced specimens.

Diagnosis. *Galapagomystides* with first segment not fused to prostomium. Trapezoidal prostomium that is dorsally "V" shaped posteriorly. Elongated dorsal cirri on segments 1, 2 and 3. Elongated ventral cirri on segment 2.

Description. Up to 25mm long, 1mm wide at segment 10 for ~60 segments. Body semi-translucent white/pink at parapodial lobes, dorsal and ventral cirri, elongated cirri, pygidial cirri, prostomium and pygidium; red in longitudinal center in life (Fig. 11,14). Trapezoidal prostomium, "V" shaped posteriorly (Fig. 12A,C & 13A); no obvious nuchal organs. Anterior dorsal edge of prostomium with paired cylindrical antennae ~0.25mm long (Fig. 12B). Paired palps ventral to antennae, similar in shape, slightly shorter (Fig. 12B). Segment one distinct from prostomium, following segments also clearly demarcated (Fig. 12A,C). Pair of elongated dorsal cirri [tentacular cirri] on each of segments 1 (~0.4mm long), 2 (~0.5mm long), 3 (~0.4mm long) (Fig. 12A,C). All elongated dorsal cirri cirriform, tapering distally. Pair of elongated ventral cirri on segment 2 (~0.2mm long) (Fig. 11B). Bulbous, rounded dorsal cirri (~0.15mm long) begin on segment 4 continuing posteriorly (Fig. 12A,D). Dorsal cirri larger than ventral cirri. Conical, tapering ventral cirri (~0.1mm long) begin on segment 3 continuing posteriorly (Fig. 12B). Ventral cilia bands present (Fig. 12B). Parapodia uniramous, notopodial chaetae absent; neuropodium with central fascicle containing ~5-8 compound chaetae; one

simple emergent acicula (Fig. 11G, 12F,G). Compound chaetal shaft cylindrical; thin, flattened pointed curled blade extended from curved joint (Fig. 11G, 12F,G). Pygidium with one pair of cirriform pygidial cirri tapering distally (~0.2mm long) (Fig. 11B,D,F).

Variation. Material examined in this study largely matches the original description (Blake and Hilbig 1990). The largest SIO-BIC specimen was 25mm long (SIO-BIC A7991, Axial seamount vents, JDF), slightly shorter than the original description at 27mm long (Blake and Hilbig 1990). *Galapagomystides verenae* specimens collected from Costa Rica and Guaymas had the similar lengths reported for the type locality.

Remarks. The specimens of *G. verenae* used in this study match the original drawing and text descriptions of *G. verenae* from the type locality published by Blake (1985). Important features include the absence of fusion between the prostomium and segment 1, the position and orientation of the elongated dorsal and ventral cirri, and lobed pygidial cirri. The first observations of living *G. verenae* have been observed here and notable is its red color as seen in other *Galapagomystides* (Fig. 11,14). Also, images of *Galapagomystides verenae* atop juvenile *Escarpia spicata* tubes from Costa Rica seeps supports the hypothesis that these worms may be blood feeders (Fig.14). Based on new genetic data and the result of our phylogenetic analysis, we move *G. verenae* from *Protomystides* to *Galapagomystides.*

Unique features for *G. verenae* include a trapezoidal prostomium that is dorsally "V" shaped posteriorly (Fig. 12A and 13A), chaetal blade length and curl (Fig. 12G and 13D), and the conical shape of ventral cirri (Fig. 12B and 13C). The total range of *G. verenae* spans from ~9°N, to ~46°N, from seeps of Guaymas Basin and Costa Rica margin to the hydrothermal vents of the Juan de Fuca Ridge. *Galapagomystides verenae* is the only member of the genus that lives at both seeps or vents (Fig. 6). *Galapagomystides verenae* is morphologically most similar to *G. patricki* n. sp. as both species show no fusion of anterior segments with the

prostomium. However, in the phylogenetic analyses, *G. verenae* was found to be the sister taxon to *G. kathyae* n. sp. (Fig. 2).

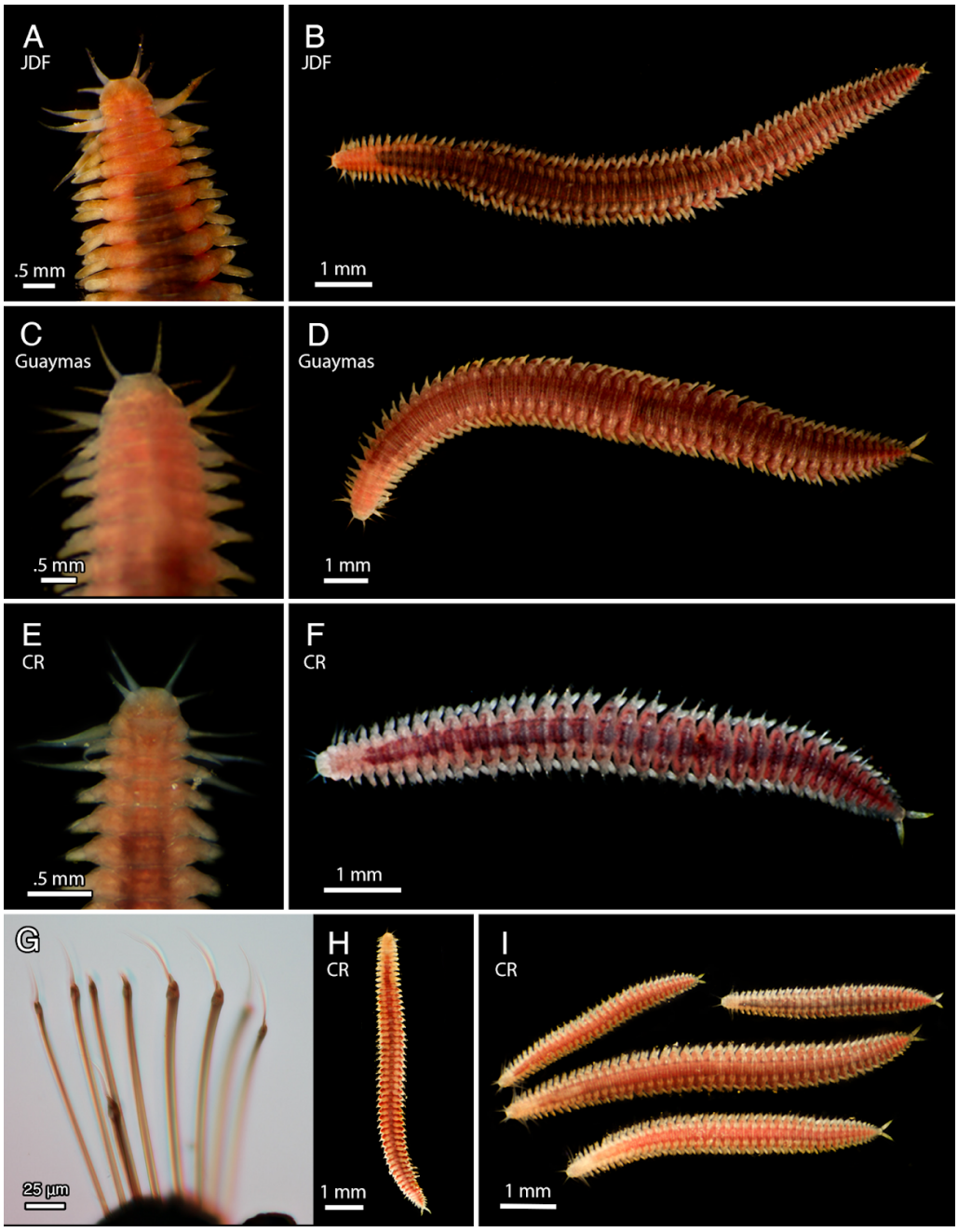

Figure 11. Photos of live *Galapagomystides verenae* from different regions. A— dorsal view of anterior (SIO-BIC A7991, Juan de Fuca Ridge). B— dorsal view of the whole worm (SIO-BIC A7991, Juan de Fuca Ridge). C— dorsal view of anterior (SIO-BIC A3263, Guaymas Basin). D— dorsal view of the whole worm (SIO-BIC A3263, Guaymas Basin). E— dorsal view of anterior (SIO-BIC A10044, Costa Rica). F— dorsal view of whole worm (SIO-BIC A10044, Costa Rica). G— compound chaetae (SIO-BIC A1830, Costa Rica). H— dorsal view of the whole worm (SIO-BIC A8466, Costa Rica). I— dorsal view of whole worms (SIO-BIC A8466, Costa Rica).

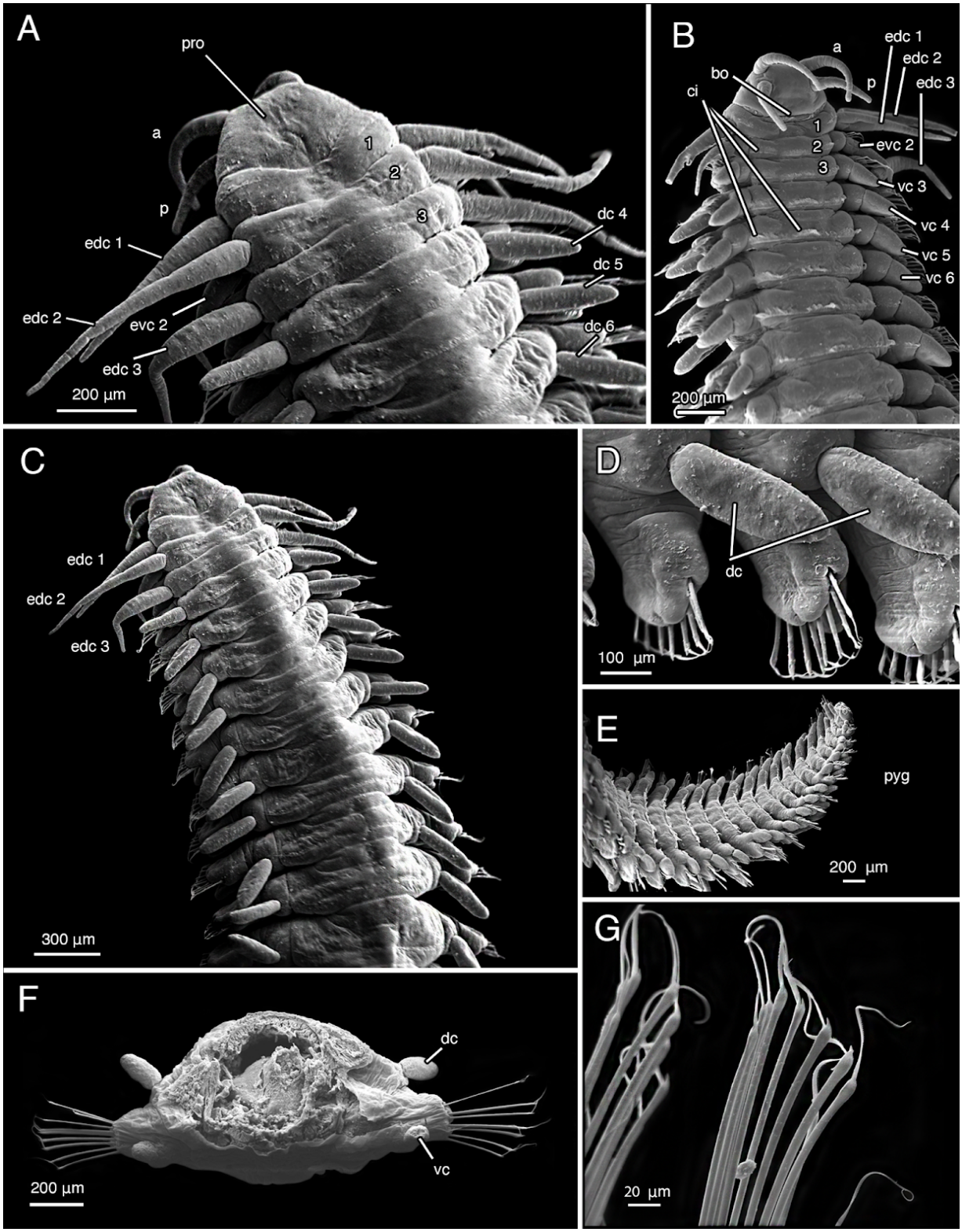

Figure 12. SEM of *Galapagomystides verenae* (SIO-BIC A7991, Juan de Fuca Ridge). A— dorsal view of anterior. B— ventral view of anterior. C— dorsal view of anterior. D— parapodia, dorsal cirri and chaetae. E— ventral/lateral view of pygidium. F— parapodia. G— compound chaetae.

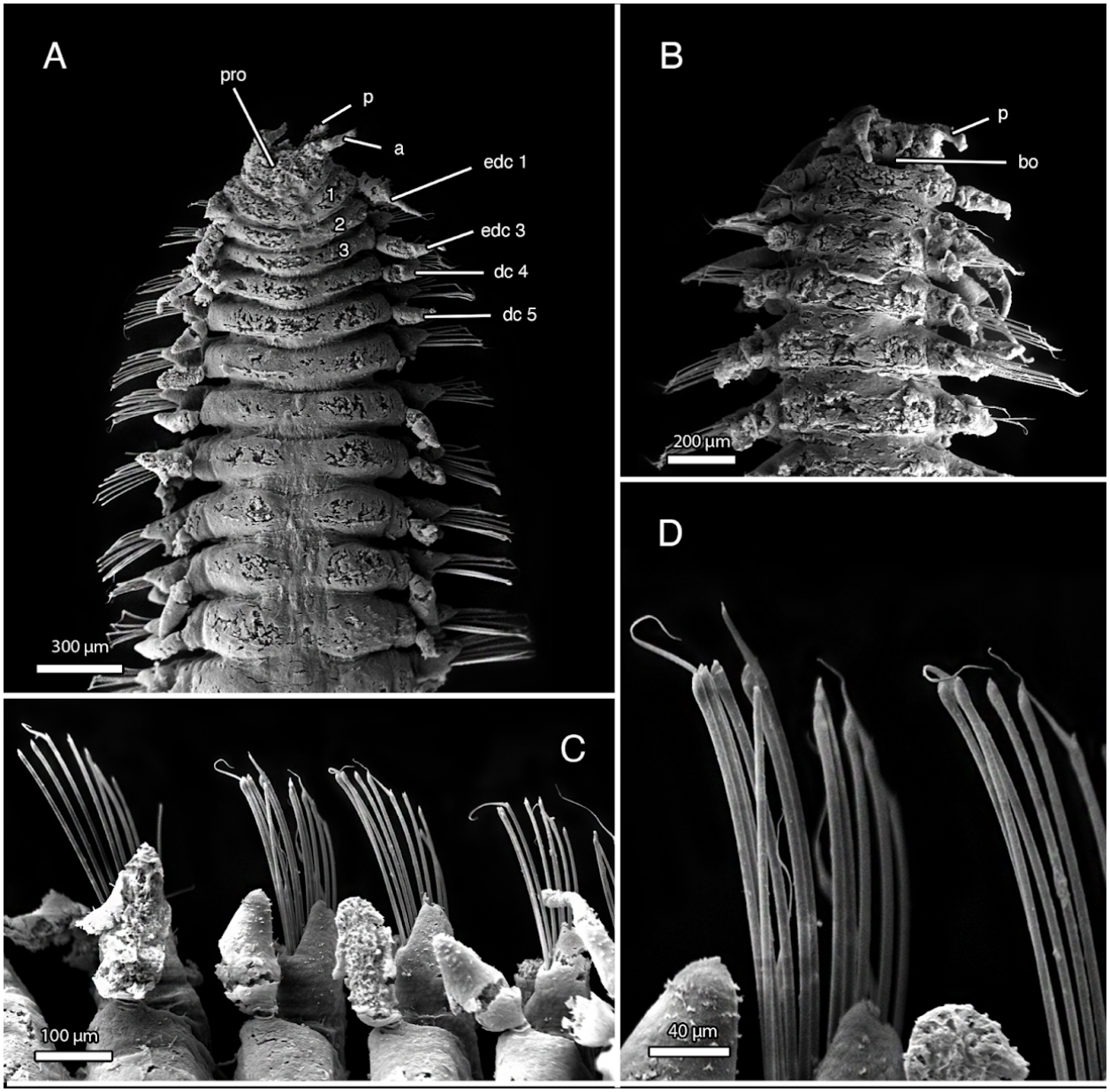

Figure 13. SEM of *Galapagomystides verenae,* paratype from the type locality (SIO-BIC A13575). A— dorsal view of anterior. B— ventral view of anterior. C— lateral view of parapodia and chaetae fascicles. D—detail of compound chaetae.

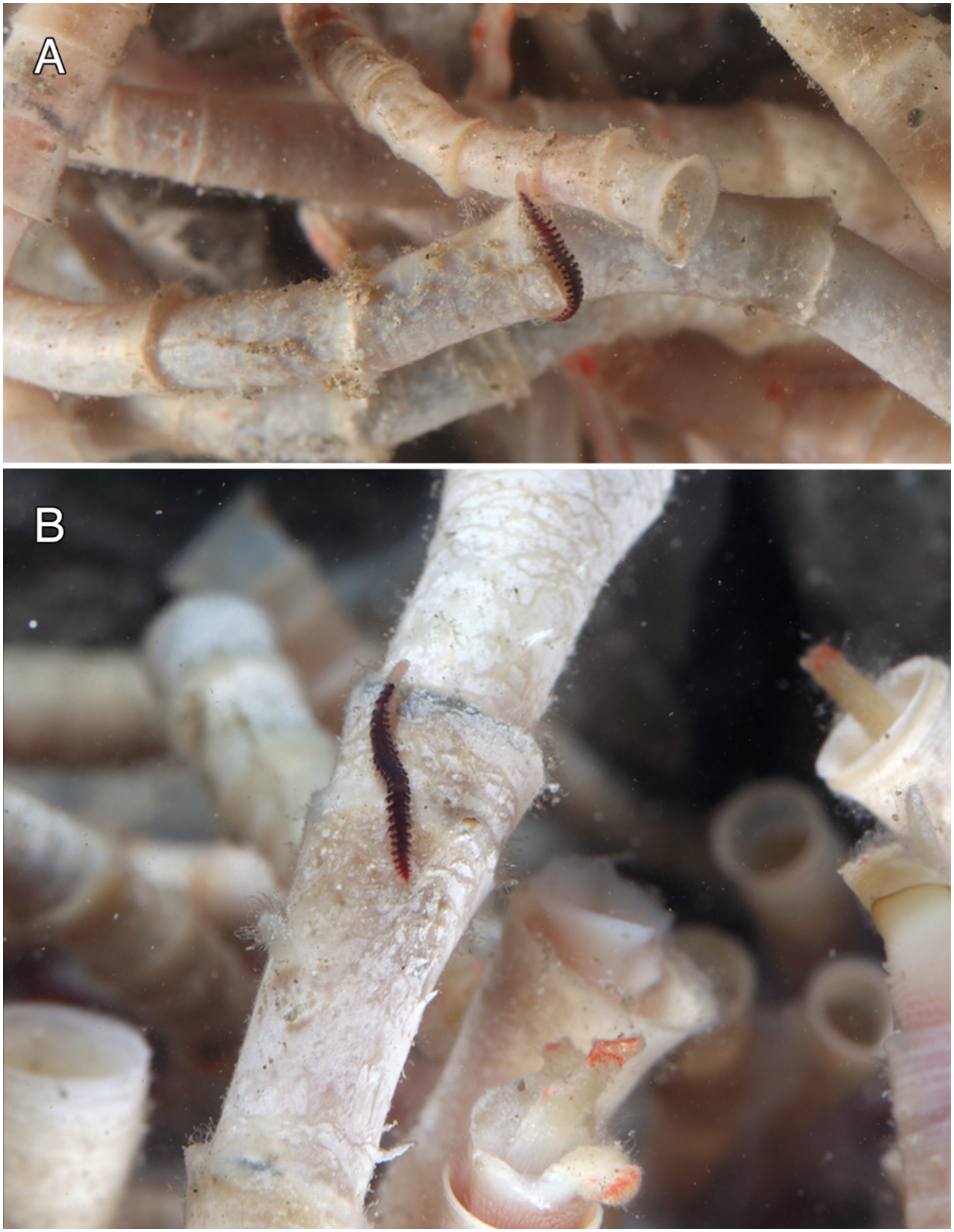

Figure 14. A & B— in situ dorsal views of *Galapagomystides verenae* associated with juvenile *Escarpia spicata* tubes at Parrita Seep off Costa Rica.

***Galapagomystides bobpearsoni* n. sp.**
Figures 15-16.

Diagnosis. First segment fused dorsally to prostomium. Elongated dorsal cirri on segments 1, 2 and 3. The elongated dorsal cirri on segments 2 and 3 are the longest of all *Galapagomystides* species. Elongated ventral cirri on segment 2.

Material Examined. Holotype: SIO-BIC A4588* (prepared for SEM), Tow Cam vent, Lau Back-arc Basin, Tonga, ~2720 meters depth, May 19, 2005, ROV Jason II. [Genbank COI= MZ711262] **Paratypes:** SIO-BIC A4590 collected from Tui Malila, Lau Back-arc Basin, Tonga, ~1890 meters depth. For locality details see Table 1. * indicates sequenced specimens.

Description. Holotype length unknown (incomplete- missing posterior end used for DNA sequencing). Body width 0.8mm at segment 10 (Fig. 15A, 16C). Body light pink/peach in life (Fig. 15C). Body brown/orange with numerous dark pigmentation speckles in preserved (formalin/ethanol) state (Fig. 15A,B). Prostomium slightly wider than long; no obvious nuchal organs (Fig. 16A,D). Anterior dorsal edge of prostomium with paired cylindrical antennae ~0.25mm long (Fig. 16A). Paired palps ventral to antennae, similar in shape and length to antennae (Fig. 16D). Segment 1 fused to prostomium, following segments clearly demarcated (Fig. 16A). Pair of elongated dorsal cirri [tentacular cirri] on each of segments 1 (~0.3mm long), 2 (~0.42mm long) and 3 (~0.44mm long) (Fig. 16A,D). All elongated dorsal cirri cirriform, tapering distally. Ventral cirri absent from segment 1 (Fig. 16D). Pair of elongated ventral cirri on segment 2 ~0.3mm long (Fig. 16D). Bulbous, rounded dorsal cirri ~0.1mm long begin on segment 3 continuing posteriorly (Fig. 16C). Cylindrical, tapering ventral cirri ~0.1mm long begin on segment 3 continuing posteriorly (Fig. 16D). Parapodia uniramous, notopodial chaetae absent; neuropodium with central fascicle containing ~5-9 compound chaetae; one simple emergent acicula (Fig. 15D,E,F,G & 16E,F). Compound chaetal shaft cylindrical; thin, flattened pointed blade extended from curved joint (Fig. 15E).

Variation. Holotype largely matches paratype. Pygidium of paratype with one pair of small lobed cirriform pygidial cirri ~ 0.2mm long rounded distally.

Remarks. *Galapagomystides bobpearsoni* n. sp. is morphologically most similar to *G. aristata* and *G. kathyae* n. sp. in having segment 1 dorsally fused to the prostomium. However, in the phylogenetic analyses, *G. bobpearsoni* n. sp. was found to be the sister group to a clade comprising *G. aristata*, *G. kathyae* n. sp. and *G. verenae*. *Galapagomystides bobpearsoni* n. sp. is restricted to Lau Back-arc Basin between 1890 -2720 meters depth. The key morphological characteristics of *G. bobpearsoni* n. sp. are the very long cirriform elongated dorsal cirri originating from the first three segments, the longest projecting from segments two and three. The chaetal blades of *G. bobpearsoni* n. sp. are the longest of all *Galapagomystides* species.

Etymology. *Galapagomystides bobpearsoni* n. sp. is named after the lead author's father, Bob Pearson, whose extreme passion and curiosity for the ocean was a major inspiration for her entry into this field.

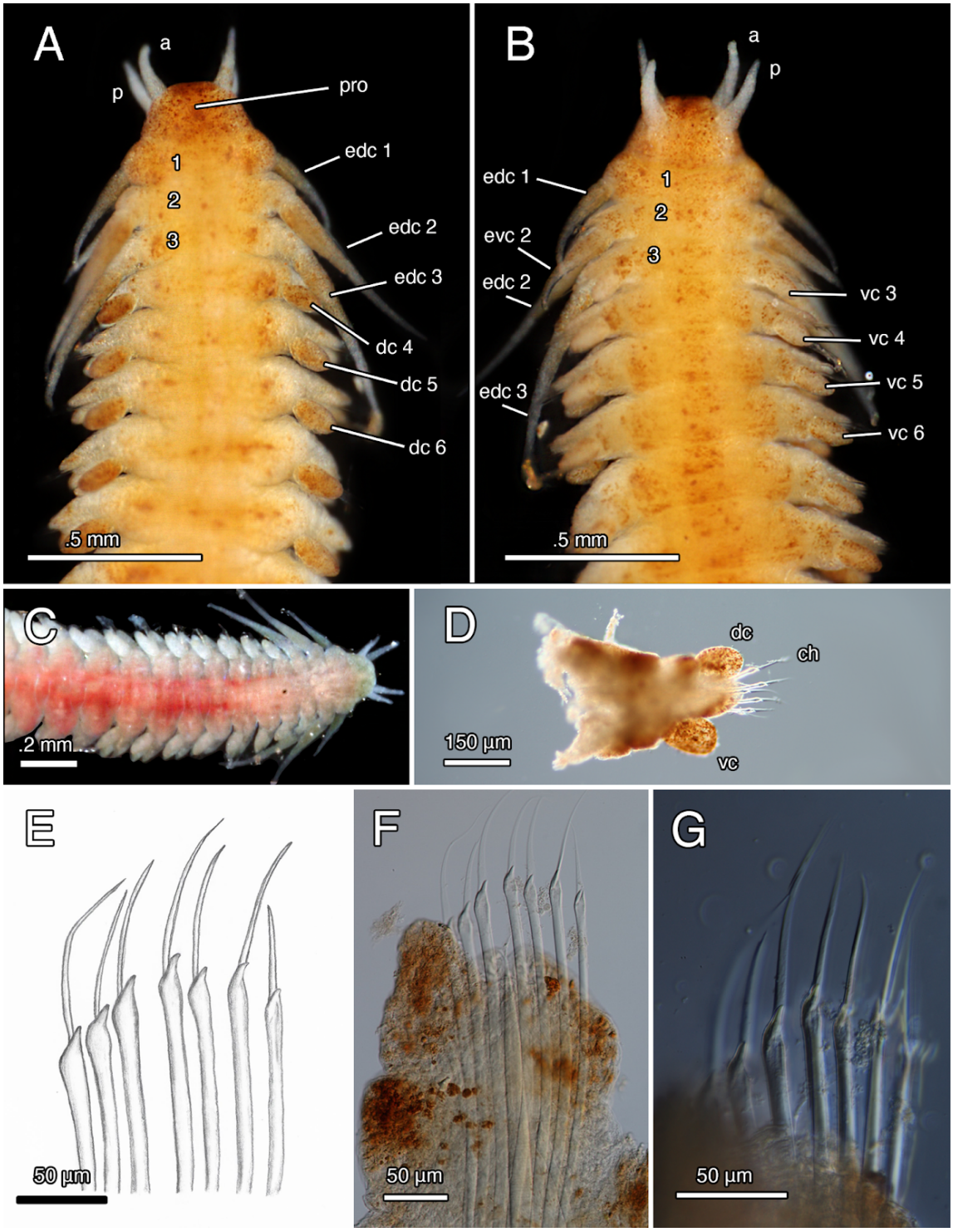

Figure 15. *Galapagomystides bobpearsoni* n. sp. holotype (SIO-BIC A4588). A— dorsal view. B— ventral view. C— dorsal view of anterior, live. D— parapodia. E—drawing of compound chaetae. F— compound chaetae. G— compound chaetae.

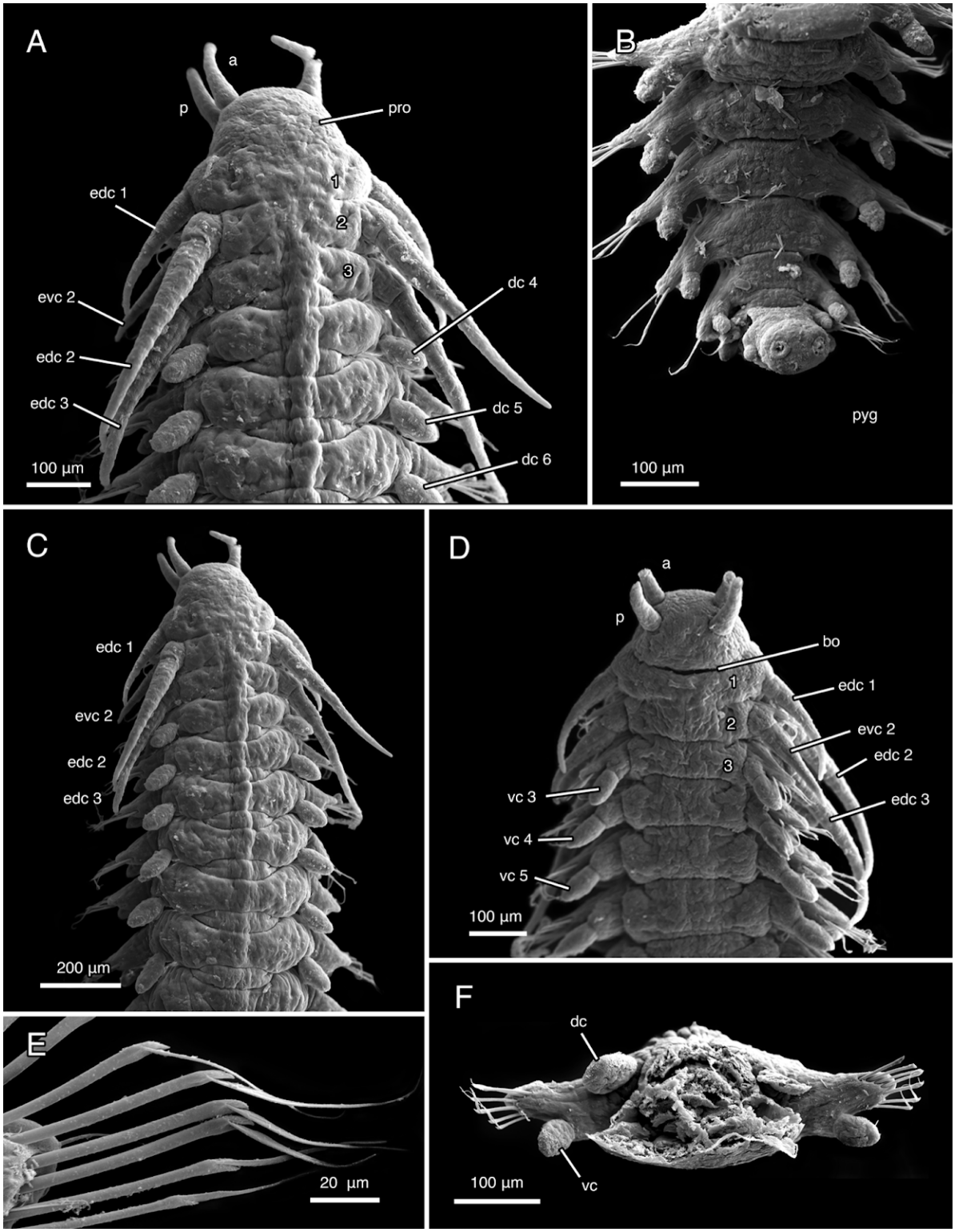

Figure 16. SEM of *Galapagomystides bobpearsoni* n. sp. A— close-up dorsal view of anterior and prostomium, holotype (SIO-BIC A4588). B— ventral view of pygidium (pygidial cirri broke off, two scars seen at distal end), paratype (SIO-BIC A4590). C— dorsal view of anterior, holotype (SIO-BIC A4588). D— ventral view of anterior (tips of antennae and palps broken off), holotype (SIO-BIC A4588). E—compound chaetae, holotype (SIO-BIC A4588). F—parapodia, holotype (SIO-BIC A4588).

***Galapagomystides kathyae* n. sp.**
Figures 17-18.

Diagnosis. First segment fused dorsally to prostomium. Wider prostomium. Elongated dorsal cirri on segments 1, 2 and 3. Elongated ventral cirri on segment 2.

Material Examined. Holotype: SIO-BIC A13418* (prepared for SEM), White Lady vent, North Fiji Basin, Fiji, 16.9905° S 173.9147° E, ~1990 meters depth, June 1, 2005, ROV Jason II. [Genbank COI= MZ711261] **Paratypes:** SIO-BIC A13422, A13423, A13424, A4651, A4645, White Lady vent, North Fiji Basin, Fiji, ~1990 meters depth; A4587, Tow Cam, Lau Back-arc Basin, Tonga, ~2720 meters depth. For locality details see Table 1. * indicates sequenced specimens.

Description. Holotype body length 14mm long, 1mm wide at segment 10 for ~65 segments. Body deep pink in life (Fig. 17C). Body brown/orange with numerous dark pigmentation speckles in preserved (formalin/ethanol) state (Fig. 17A,B,D). Lobe-like prostomium; no obvious nuchal organs (Fig. 18A). Anterior dorsal edge of prostomium with paired cylindrical antennae ~0.2mm long (Fig. 18A,D). Paired palps ventral to antennae, similar in shape and length to antennae (Fig. 18,D). Segment one dorsally fused to prostomium, following segments clearly demarcated (Fig. 18A). Pair of elongated dorsal cirri [tentacular cirri] on each of segments 1 (~0.25mm long), 2 (~0.25mm long) and 3 (~0.2mm long) (Fig. 18A). All elongated dorsal cirri cirriform, tapering distally. Pair of elongated ventral cirri on segment 2 ~0.15mm long (Fig. 18D). Bulbous, rounded dorsal cirri ~0.08mm long begin on segment 4 continuing posteriorly (Fig. 18A,C). Conical, tapering ventral cirri ~0.1mm long begin on segment 3 continuing posteriorly (Fig. 18D). Ventral cilia bands present (Fig. 18D). Parapodia uniramous, notopodial chaetae absent; neuropodium with central fascicle containing ~5-8 compound chaetae; one simple emergent acicula (Fig. 17E,F,G & 18F). Compound chaetal

shaft cylindrical; thin, flattened pointed blade extended from curved joint (Fig. 17E). Pygidium with one pair of small lobed cirriform pygidial cirri ~0.1mm long rounded distally (Fig. 18B).

Variation. Paratypes largely match the holotype. The paratype SIO-BIC A4651 of *G. kathyae* n. sp. is a juvenile (Fig. 17D), has less segments and is smaller than the holotype. This specimen was not sequenced but the morphology matches the holotype.

Remarks. *Galapagomystides kathyae* n. sp. is morphologically most similar to *G. aristata* and *G. bobpearsoni* n. sp. in which all have segment 1 dorsally fused to the prostomium. However, in the phylogenetic analyses, *G. kathyae* n. sp. was the sister group to *G. verenae* (Fig. 2). *Galapagomystides kathyae* n. sp. was found at both the North Fiji Basin and Lau Back-arc Basin, separated by a distance of 1110 km. The single specimen collected from the Lau Back-arc Basin does not have a DNA sequence, but was morphologically similar to the holotype. The distinguishing morphological characteristics of *G. kathyae* n. sp. are a wide prostomium, and elongated dorsal cirri originating from the second segment having a signature 90° angle distal to the body. The chaetal blades of *G. kathyae* n. sp. are thin and appear delicate, originating from a pointed joint.

Etymology. *Galapagomystides kathyae* n. sp. is named after the lead author's mother, Kathy Reimer-Pearson, who sparked the lead-author's interest in invertebrates and the natural world during babyhood.

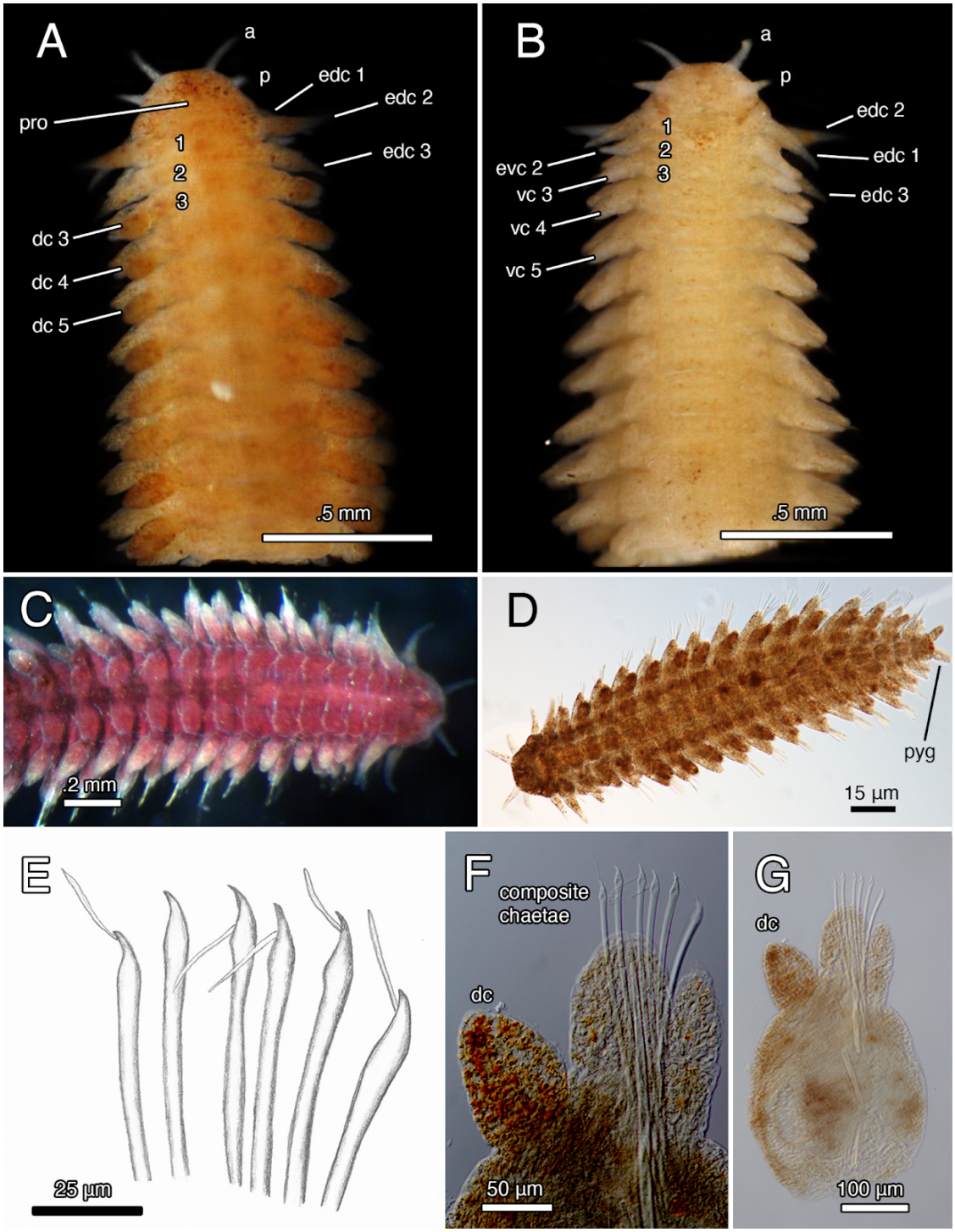

Figure 17. color photos of *Galapagomystides kathyae* n. sp. A— dorsal view, holotype (SIO-BIC A13418). B— ventral view of holotype, holotype (SIO-BIC A13418). C— live dorsal view, holotype (SIO-BIC A13418). D—whole body, paratype (SIO-BIC A4651). E— drawing of compound chaetae, holotype (SIO-BIC A13418). F— dorsal cirri, holotype (SIO-BIC A13418). G— parapodia, holotype (SIO-BIC A13418).

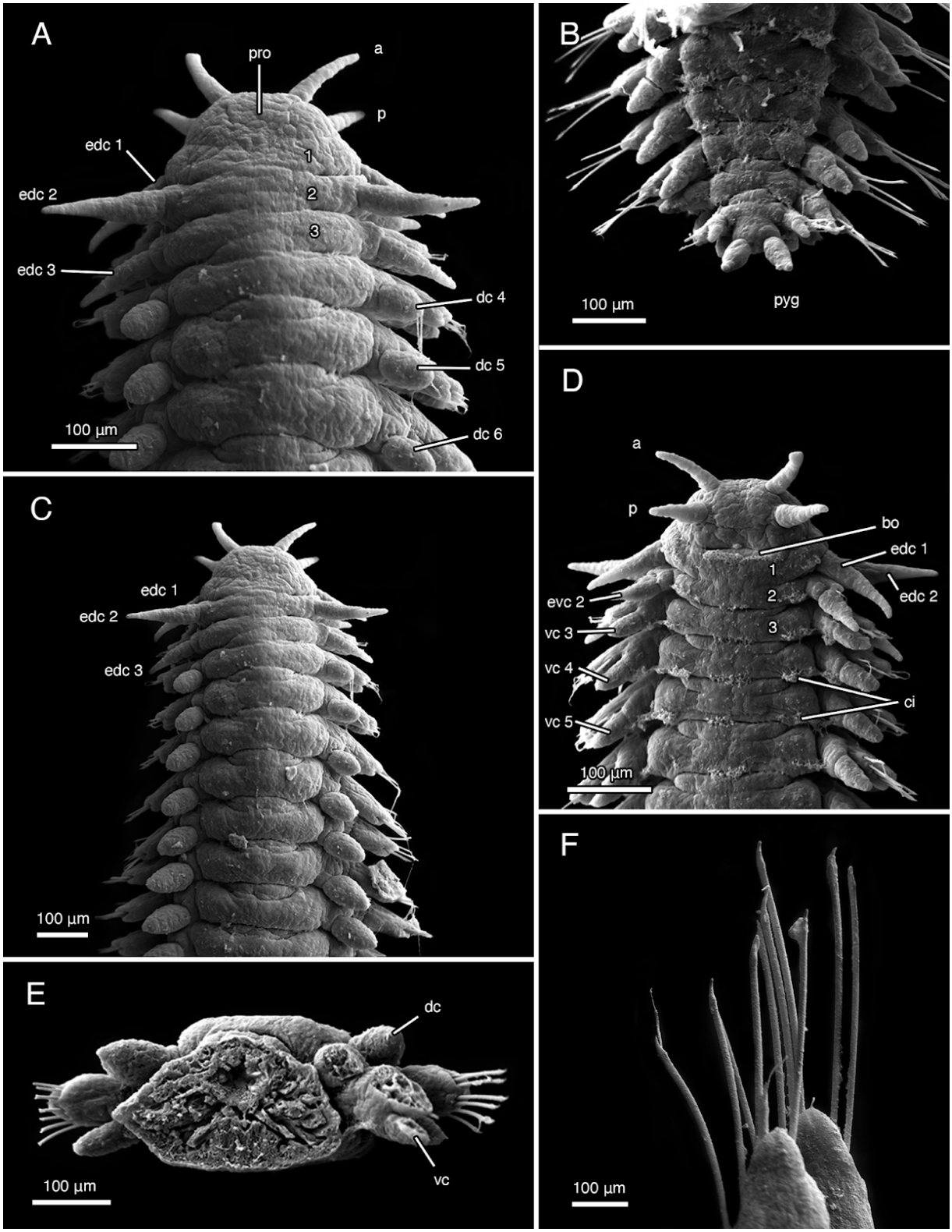

Figure 18. SEM of *Galapagomystides kathyae* n. sp. holotype (SIO-BIC A13418). A— close-up dorsal view of anterior and prostomium. B— ventral view of pygidium with pygidial cirri. C— dorsal view of anterior. D— ventral view of anterior. E—parapodia. F—compound chaetae.

***Galapagomystides patricki* n. sp.**
Figures 19-20.

Diagnosis. First segment not fused to prostomium. Elongated dorsal cirri on segments 1 and 2. No elongated ventral cirri.

Material Examined. Holotype: SIO-BIC A13419* (prepared for SEM), Parrita Seep, Costa Rica; 9.0303° N 84.623° W, ~1415 meters depth, March 1, 2009, HOV Alvin. [Genbank COI= MZ711314] **Paratypes:** SIO-BIC: A13425, A13426, A13427, A13420*, A13421*, Parrita Seep, Costa Rica ~1400 meters depth; SIO-BIC: A9964*, A9875*, A9877*, A9947* (MZUCR), A9961*, A9934, Jacó Scar, Costa Rica, ~1770 meters depth; SIO-BIC: A1424, ~20km away Parrita Seep, unknown depth. For locality details see Table 1. * indicates sequenced specimens.

Description. Holotype body length 16mm, 1mm wide at segment 10 for ~70 segments. Body mauve in life (Fig. 19A). Body brown/orange with numerous dark pigmentation speckles in preserved (formalin/ethanol) state (Fig. 19C,D). Lobe-like prostomium; no obvious nuchal organs (Fig. 20A). Anterior dorsal edge of prostomium with paired cylindrical antennae (~0.25mm long) (Fig. 20A). Paired palps ventral to antennae, similar in shape and length to antennae (Fig. 20D). Segment one not fused to prostomium, distinct dorsally and ventrally, following segments clearly demarcated (Fig. 20A,C). Pair of elongated dorsal cirri [tentacular cirri] on each of segments 1 (~0.4 long), 2 (~0.35mm long) (Fig. 20A). All elongated dorsal cirri cirriform, tapering distally (Fig. 20A). No elongated ventral cirri (Fig. 20D). Segment 3 lacking dorsal cirri (Figs 19B, C, 20A). Bulbous, rounded dorsal cirri (~0.1mm long) begin on segment 4 continuing posteriorly (Fig. 20C). Ventral cirri absent on segment 1(Fig. 20D). Bulbous ventral cirri (~.05mm long) (Fig. 20D). Chaetae begin on segment 2 continuing posteriorly (Fig. 20A). Parapodia uniramous, notopodial chaetae absent; neuropodium with central fascicle containing ~6-10 compound chaetae; one simple emergent acicula (Fig. 19E,F,G,H & 20F). Compound

chaetal shaft cylindrical; thin, flattened triangular short blade extending from rounded joint (Fig. 19E & 20F). Pygidium with one pair of lobed pygidial cirri (~0.15mm long) rounded distally (Fig. 20B).

Variation. Most *G. patricki* n. sp. type material specimens were within +/- 1 to 3 millimeters from the holotype in overall length, though one juvenile was ~10mm smaller than the holotype. The specimens ranged from ~40 segments to ~70 segments. Paratypes of *G. patricki* n. sp. vary in color with body semi-translucent white/pink at parapodial lobes, dorsal and ventral cirri, prostomium and pygidium; red in longitudinal center; yellow patch on prostomium; yellow-white elongated cirri and pygidial cirri in life (Fig. 19B). Palps and antennae on paratypes are tapered. Some incomplete samples. All other considerations largely match the holotype.

Remarks. Most *G. patricki* n. sp. samples were collected from Parrita Seep, Costa Rica (1400 m.), excepting one specimen collected from the deeper Jacó Scar, Costa Rica (1800 m.). A single sample, A1424, was collected from a multicore that was deployed offsite in the vicinity of the seep. Some *G. patricki* n. sp. were found forming sandy tubes inside empty vestimentiferan tubes. Morphologically, *G. patricki* n. sp. is most similar to *G. verenae* as both species show no fusion of anterior segments with the prostomium. However, in the phylogenetic analyses, *G. patricki* n. sp. was the sister group to the rest of the genus (Fig. 2). *Galapagomystidespatricki* n. sp. lacks dorsal cirri on segment three (all other species have either elongated or regular dorsal cirri on segment three). The chaetae of *G. patricki* n. sp. have the shortest blades compared to other species, and are also triangular in shape (while the blades in other species are falcate). *Dorsal elongated cirri on segment one, right side and dorsal elongated cirri on segment two, left side have broken off of holotype.

Etymology: *Galapagomystides patricki* n. sp. is named after Patrick Shaughnessy, whose support during this project was instrumental to the lead author's success.

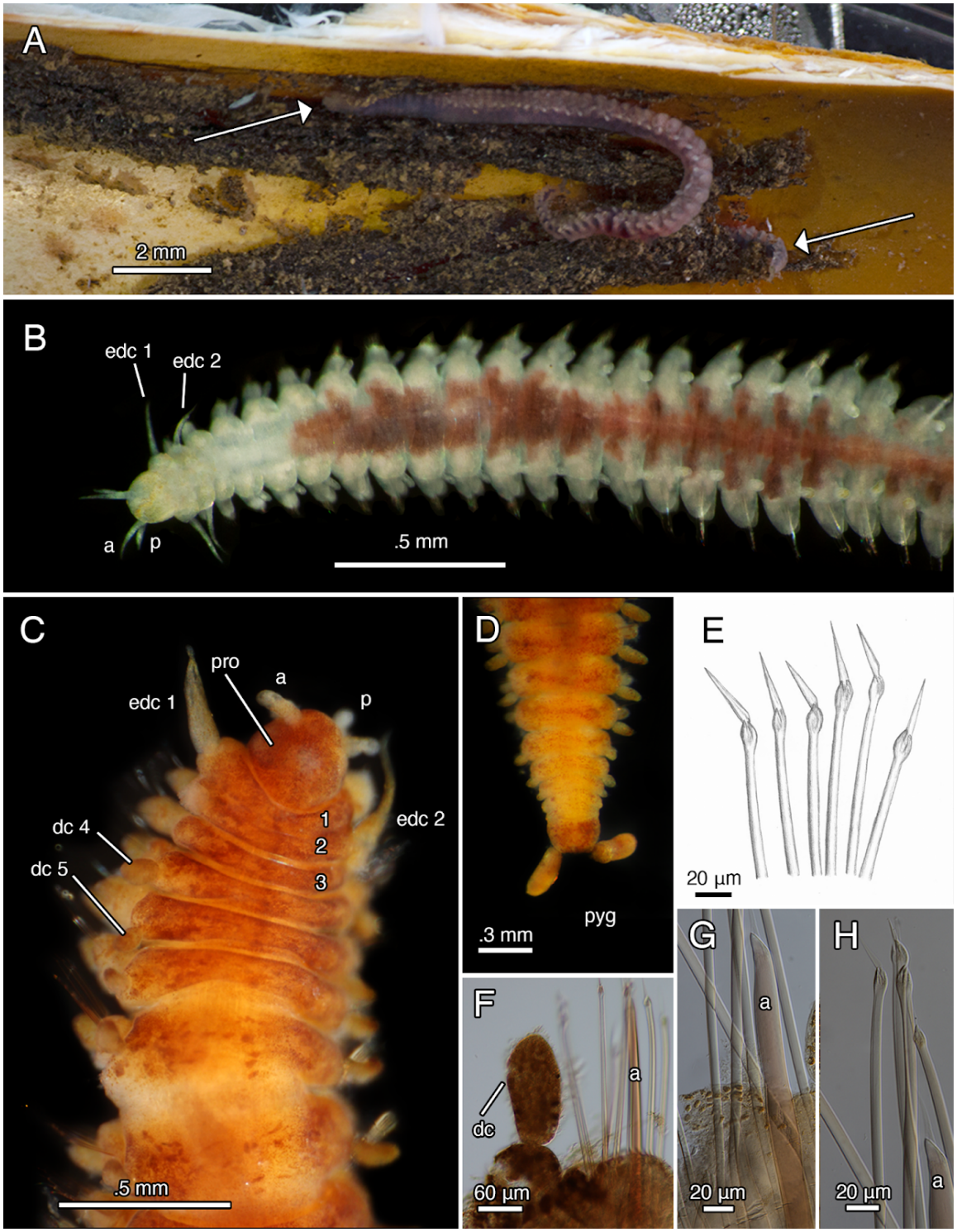

Figure 19. *Galapagomystides patricki* n. sp. A— *in situ Galapagomystides* inside Vestimentiferan tube, Alvin Dive 4508, Mound Quepos, Parrita Seep, Costa Rica, paratype (SIO-BIC A13420; A13420). B—dorsal view of anterior, paratype (SIO-BIC A1424). C— dorsal view of anterior and prostomium, holotype (SIO-BIC A13419). D— dorsal view of pygidium with pygidial cirri, holotype (SIO-BIC A13419). E—drawing of compound chaetae, holotype (SIO-BIC A13419). F— dorsal cirri, holotype (SIO-BIC A13419). G— aciculum, holotype (SIO-BIC A13419). H— compound cirri, holotype (SIO-BIC A13419).

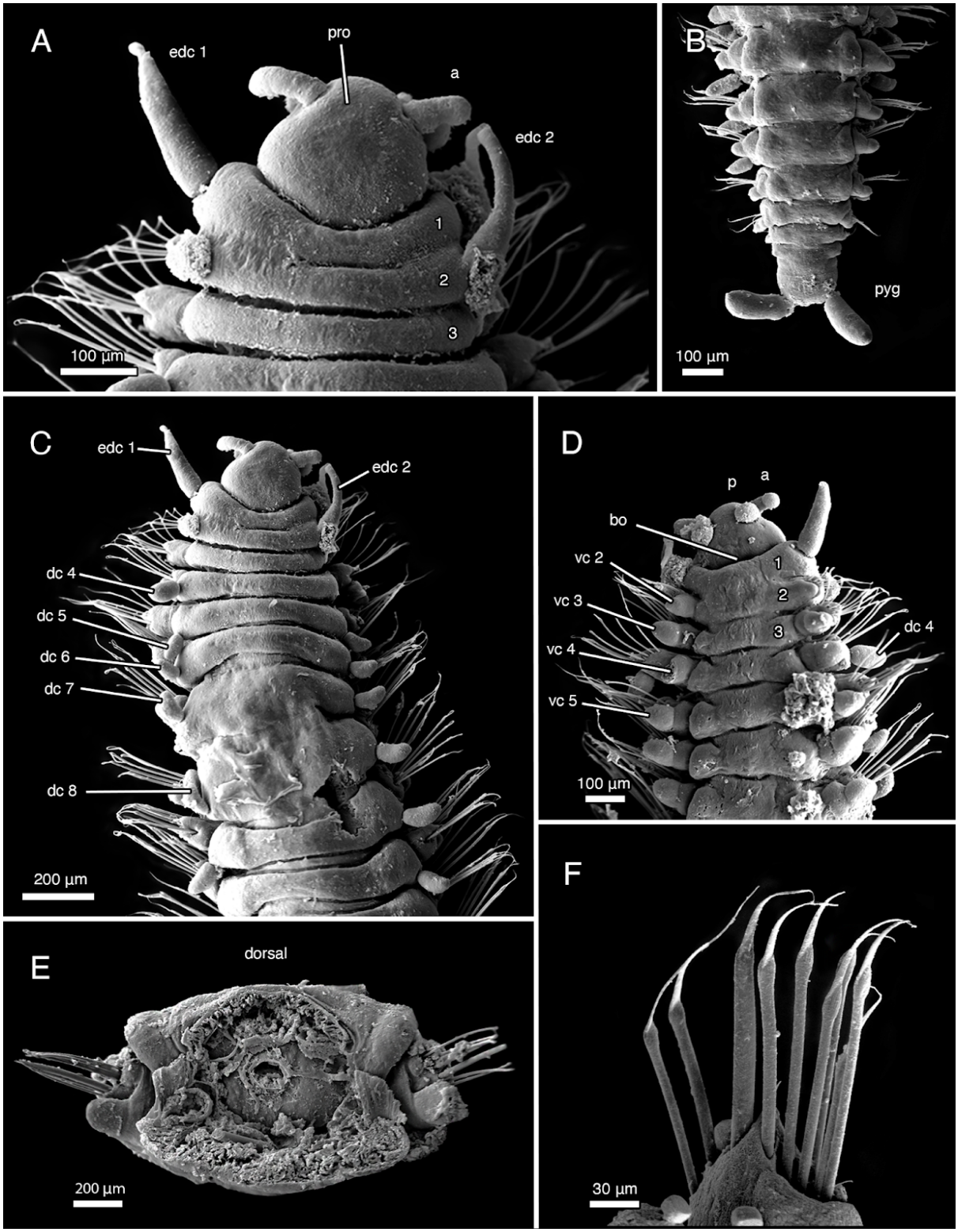

Figure 20. SEM of *Galapagomystides patricki* n. sp. holotype (SIO-BIC A13419). A— close-up dorsal view of anterior and prostomium. B— dorsal view of pygidium with pygidial cirri. C— dorsal view of anterior. D— ventral view of anterior. E—parapodia. F—compound chaetae.

Supporting Data

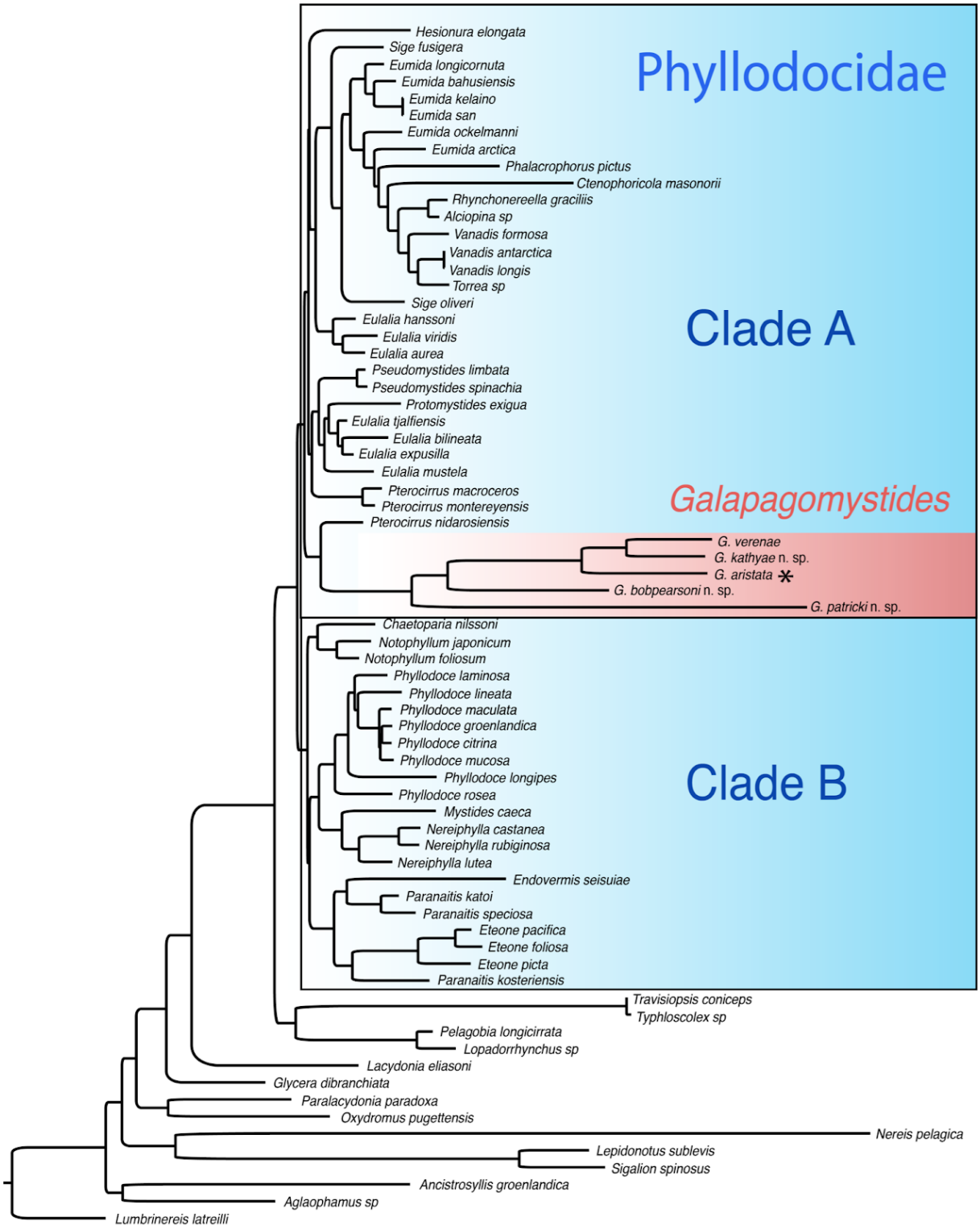

Figure 21. Maximum Likelihood (ML) tree rendered from the concatenation of genes COI, 18S, 28S and 16S including outgroups (unshaded) to show supportive phylogeny. '*' indicates type species.

This manuscript is coauthored with Dr. Greg Rouse. The thesis author was the primary author of this manuscript.

References

Bandelt, H.J., Forster, P. & Röhl, A. (1999) Median-joining networks for inferring intraspecific phylogenies. *Molecular biology and evolution* 16, 37–48. https://doi.org/10.1093/oxfordjournals.molbev.a026036

Becker, E.L., Cordes, E.E., Macko, S. A., Lee, R.W., & Fisher, C.R. (2013) Using stable isotope compositions of animal tissues to infer trophic interactions in gulf of mexico lower slope seep communities. *PloS One* 8, e74459. https://doi.org/10.1371/journal.pone.0074459

Bergquist, D.C., Eckner, J.T., Urcuyo, I.A. , Cordes, E.E., Hourdez, S., Macko, S.A., & Fisher, C.R. (2007) Using stable isotopes and quantitative community characteristics to determine a local hydrothermal vent food web. *Marine Ecology Progress Series*, 330, 49–65. https://doi.org/10.3354/meps330049

Black, M.B., Halanych, K.M., Maas, P.A.Y., Hoeh, W.R., Hashimoto, J., Desbruyères, D., Lutz, R.A., & Vrijenhoek, R.C. (1997) Molecular systematics of vestimentiferan tubeworms from hydrothermal vents and cold-water seeps. *Marine Biology*, 130, 141–49. https://doi.org/10.1007/s002270050233

Blake, J.A. (1985) Polychaeta from the vicinity of deep-sea geothermal vents in the eastern pacific. I. Euphrosinidae, Phyllodocidae, Hesionidae, Nereididae, Glyceridae, Dorvilleidae, Orbiniidae, and Maldanidae. *Bulletin of the Biological Society of Washington*, 6, 67–101.

Blake, J.A. (1994) Family phyllodocidae Savigny, 1818. *In:* Blake, J.A. & Hilbig, B. (Ed.), *Taxonomic Atlas of the Benthic Fauna of the Santa Maria Basin and Western Santa Barbara Channel. Vol. 4. The Annelida, Part 2.* Science Applications International Corporation, Woods Hole, pp. 115–86.

Blake, J.A., & Hilbig, B. (1990) Polychaeta from the vicinity of deep-sea hydrothermal vents in the eastern pacific. II. New Species and Records from the Juan de Fuca and Explorer Ridge Systems. *Pacific Science*, 44, 219–253

Borda, E., Kudenov, J.D., Chevaldonné, P., Blake, J.A., Desbruyères, D., Fabri, M.C., Hourdez, S., Pleijel, F., Shank, T.M., Wilson, N.G., Schulze, A., & Rouse, G.W. (2013) Cryptic species of *Archinome* (Annelida: Amphinomida) from vents and seeps. *Proceedings. Biological*

Sciences: The Royal Society, 280, 20131876. https://doi.org/10.1098/rspb.2013.1876

Carr, C.M., Hardy, S.M., Brown, T.M., Macdonald, T.A. & Hebert, P.D.N. (2011) A tri-oceanic perspective: DNA barcoding reveals geographic structure and cryptic diversity in canadian Polychaetes. *PloS One* 6, e22232. https://doi.org/10.1371/journal.pone.0022232

Chapman, A.S.A., Tunnicliffe, V., & Bates, A.E. (2018) Both rare and common species make unique contributions to functional diversity in an ecosystem unaffected by human activities. *Diversity & Distributions*, 24, 568–78. https://doi.org/10.1111/ddi.12712

Chevaldonné, P., Jollivet, D., Desbruyères, D., Lutz, R., & Vrijenhoek, R. (2002) Sister-species of eastern Pacific hydrothermal vent worms (Ampharetidae, Alvinellidae, Vestimentifera) provide new mitochondrial COI clock calibration. *CBM-Cahiers de Biologie Marine*, 43, 367–370.

Darriba, D., Posada, D., Kozlov, A.M., Stamatakis, A., Morel, B., & Flouri, T. (2020) ModelTest-NG: a new and scalable tool for the selection of DNA and protein evolutionary models. *Molecular Biology and Evolution*, 37, 291–94. https://doi.org/10.1093/molbev/msz189

Desbruyères, D., & Segonzac, M. (1997) *Handbook of deep-sea hydrothermal vent fauna*. IFREMER, Brest, France.

Desbruyères, D., Segonzac, M., & Bright, M. Eds. (2006) *Handbook of deep-sea hydrothermal vent fauna*. Denisia, Linz, Austria.

Dreyer, J.C. (2004) Stability at hydrothermal-vent mussel beds: dynamics at hydrothermal vents: evidence for stable macrofaunal communities in mussel beds on the northern East Pacific Rise. Available from: https://dx.doi.org/doi:10.21220/s2-e641-wn93 (accessed 28 september 2021)

Edler, D., Klein, J., Antonelli, A., & Silvestro, D. (2021) raxmlGUI 2.0: A graphical interface and toolkit for phylogenetic analyses using RAxML. *Methods in Ecology and Evolution*, 12, 373–77.

https://doi.org/10.1111/2041-210X.13512

Eklöf, J., Pleijel, F., & Sundberg, P. (2007) Phylogeny of benthic phyllodocidae (polychaeta) based on morphological and molecular data. *Molecular Phylogenetics and Evolution*, 45, 261–71. https://doi.org/10.1016/j.ympev.2007.04.015

Giribet, G., S. Carranza, J. Baguna, M. Riutort, & C. Ribera. (1996) First molecular evidence for the existence of a tardigrada arthropoda clade. *Molecular Biology and Evolution*, 13, 76–84. https://doi.org/10.1093/oxfordjournals.molbev.a025573.

Gollner, S., Govenar, B., Fisher, C.R., & Bright, M. (2015) Size matters at deep-sea hydrothermal vents: different diversity and habitat fidelity patterns of meio- and macrofauna. *Marine Ecology Progress Series*, 520, 57–66. https://doi.org/10.3354/meps11078

Govenar, B.W., Bergquist, D.C. Istvan, Urcuyo, A., Eckner, J.T. & Fisher, C.R. (2002) Three *Ridgeia Piscesae* assemblages from a single Juan de Fuca ridge sulphide edifice: structurally different and functionally similar. *Cahiers de Biologie Marine*, 43, 247–52.

Govenar, B., Freeman, M., Bergquist, D.C., Johnson, G.A., & Fisher, C.R. (2004) Composition of a one-year-old *Riftia Pachyptila* community following a clearance experiment: insight to succession patterns at deep-sea hydrothermal vents. *The Biological Bulletin*, 207, 177–82. https://doi.org/10.2307/1543204

Govenar, B., Le Bris, N., Gollner, S., Glanville, J., Aperghis, A.B. , Hourdez, S. & Fisher, C.R. (2005) Epifaunal community structure associated with *Riftia Pachyptila* aggregations in chemically different hydrothermal vent habitats. *Marine Ecology Progress Series*, 305, 67–77. https://doi.org/10.3354/meps305067

Govenar, B. & Fisher, C.R. (2007) Experimental evidence of habitat provision by aggregations of *Riftia Pachyptila* at hydrothermal vents on the East Pacific Rise. *Marine Ecology*, 28, 3–14. https://doi.org/10.1111/j.1439-0485.2007.00148.x

Hartman, O. (1936) A review of the Phyllodocidae (Annelida Polychaeta) of the coast of California, with descriptions of nine new species. *University of California Publications in*

Zoology, 41, 117–132.

Hatch, A.S., Liew, H., Hourdez, S., & Rouse, G.W. (2020) Hungry scale worms: phylogenetics of *Peinaleopolynoe* (Polynoidae, Annelida), with four new species. *ZooKeys*, 932, 27–74. https://doi.org/10.3897/zookeys.932.48532

Imajima, M. (2001) Deep-sea benthic polychaetous annelids of Tosa Bay, southwestern Japan. *National Science Museum Monographs*, 20, 31–100.

Jenkins, C.D., Ward, M.E., Turnipseed, M., Osterberg, J., & Van Dover, C.L. (2002) The digestive system of the hydrothermal vent polychaete *Galapagomystides aristata* (Phyllodocidae): evidence for hematophagy? *Invertebrate Biology*, 121, 243–254. https://doi.org/10.1111/j.1744-7410.2002.tb00064.x

Jimi, N., Kimura, T., Ogawa, A., & Kajihara, H. (2020) Alien worm in worm: a new genus of endoparasitic polychaete (Phyllodocidae, Annelida) from scale worms (Aphroditidae and Polynoidae, Annelida). *Systematics and Biodiversity*, 19, 13–21. https://doi.org/10.1080/14772000.2020.1785038

Katoh, K., & Standley, D.M. (2013) MAFFT multiple sequence alignment software version 7: improvements in performance and usability. *Molecular Biology and Evolution*, 30, 772–80. https://doi.org/10.1093/molbev/mst010

Kearse, M., Moir, R., Wilson, A., Stones-Havas, S., Cheung, M., Sturrock, S., Buxton, S., Cooper, A., Markowitz, S., Duran, C. & Thierer, T. (2012) Geneious basic: an integrated and extendable desktop software platform for the organization and analysis of sequence data. *Bioinformatics*, 28, 1647–49. https://doi.org/10.1093/bioinformatics/bts199

Kelly, N., Metaxas, A., & Butterfield, D. (2007) Spatial and temporal patterns of colonization by deep-sea hydrothermal vent invertebrates on the Juan de Fuca Ridge, NE Pacific. *Aquatic Biology*, 1, 1–16. https://doi.org/10.3354/ab00001

Kiel, S. (2016) A biogeographic network reveals evolutionary links between deep-sea hydrothermal vent and methane seep faunas. *Proceedings. Biological Sciences: The Royal*

Society, 283, 2016–2337. http://dx.doi.org/10.1098/rspb.2016.2337

Kobayashi, G. & Kojima, S. (2017) First record of *Protomystides Hatsushimaensis* (Annelida: Phyllodocidae) inhabiting vacant tubes of vestimentiferan tubeworms. *Marine Biodiversity Records*, 10, 25. https://doi.org/10.1186/s41200-017-0127-9

Kozlov, M.A., Darriba, D., Flouri, T., Morel, B., & Stamatakis, A. (2019) RAxML-NG: A fast, scalable and user-friendly tool for maximum likelihood phylogenetic inference. *Bioinformatics*, 35, 4453–4455. https://doi.org/10.1093/bioinformatics/btz305

Krylova, E.M., & Sahling, H. (2010) Vesicomyidae (bivalvia): current taxonomy and distribution. *PloS One* 5, e9957. https://doi.org/10.1371/journal.pone.0009957

Le, H.L., Lecointre, G., & Perasso, R. (1993) A 28S rRNA-based phylogeny of the gnathostomes: first steps in the analysis of conflict and congruence with morphologically based cladograms. *Molecular Phylogenetics and Evolution*, 2, 31–51. https://doi.org/10.1006/mpev.1993.1005

Leigh, J.W., Bryant, D., & Nakagawa, S. (2015) POPART: full-feature software for haplotype network construction. *Methods in Ecology and Evolution*, 6, 1110–1116. https://doi.org/10.1111/2041-210X.12410

Leiva, C., Riesgo, A., Avila, C., Rouse, G.W., & Taboada, S. (2018) Population structure and phylogenetic relationships of a new shallow-water antarctic Phyllodocid Annelid. *Zoologica Scripta*, 47, 714–26. https://doi.org/10.1111/zsc.12313

Lelièvre, Y., Sarrazin, J., Marticorena, J., Schaal, G., Day, T., Legendre, P., Hourdez, S., & Matabos, M. (2017) Biodiversity and trophic ecology of hydrothermal vent fauna associated with tubeworm assemblages on the Juan de Fuca Ridge. *Biogeosciences Discussions*, 1–34. https://doi.org/10.5194/bg-2017-411

Levin, L.A., Baco, A.R., Bowden, D.A., Colaco, A., Cordes, E.E., Cunha, M.R., Demopoulos, A.W., Gobin, J., Grupe, B.M., Le, J. & Metaxas, A. (2016) Hydrothermal vents and methane seeps: rethinking the sphere of influence. *Frontiers in Marine Science*, 3, 72.

https://doi.org/10.3389/fmars.2016.00072

Lewis, P.O. (2001) A likelihood approach to estimating phylogeny from discrete morphological character data. *Systematic Biology*, 50, 913–25. https://doi.org/10.1080/106351501753462876

Lockyer, A.E., Olson, P.D., & Littlewood, D.T.J. (2003) Utility of complete large and small subunit rRNA genes in resolving the phylogeny of the Neodermata (Platyhelminthes): Implications and a review of the cercomer theory. *Biological Journal of the Linnean Society*, 78, 155–71. https://doi.org/10.1046/j.1095-8312.2003.00141.x

Maddison, W.P. & Maddison, D.R. (2019) Mesquite: a modular system for evolutionary analysis. Version 3.61. Available from: http://www.mesquiteproject.org (accessed 28 September 2021)

Marcus, J. & Anholt, B.R. (2003) Nonrandom species patterns in hydrothermal vent survey data: a null model approach. *Community ecology of hydrothermal vents at Aiial Volcano, Juan de Fuca Ridge, northeast PaciGc*, 18.

McCowin, M.F., Feehery, C., & Rouse, G.W. (2020) Spanning the depths or depth-restricted: three new species of *Bathymodiolus* (Bivalvia, Mytilidae) and a new record for the hydrothermal vent *Bathymodiolus Thermophilus* at methane seeps along the Costa Rica Margin. *Deep Sea Research Part I: Oceanographic Research Papers*, 164, 103–322. https://doi.org/10.1016/j.dsr.2020.103322

McCowin, M.F., & Rouse, G.W. (2018) A New *Lamellibrachia* species and confirmed range extension for *Lamellibrachia Barhami* (Siboglinidae, Annelida) from Costa Rica methane seeps. *Zootaxa*, 4504, 1–22. https://doi.org/10.11646/zootaxa.4504.1.1

Milligan, B.N., & Tunnicliffe, V. (1994) Vent and nonvent faunas of Cleft Segment, Juan de Fuca Ridge, and their relations to lava age. *Journal of Geophysical Research,* 99, 4777–4786. https://doi.org/10.1029/93JB03210

Miura, T. (1988) A new species of the genus *Protomystides* (Annelida, Polychaeta) associated

with a Vestimentiferan worm from the Hatsushima Cold-Seep site. *Japanese Society of Systematic Zoology*, 38, 10–14.

Muir, A. & Maruf Hossain, M.M. (2014) The intertidal polychaete (Annelida) fauna of the Sitakunda coast (Chittagong, Bangladesh), with notes on the Capitellidae, Glyceridae, Lumbrineridae, Nephtyidae, Nereididae and Phyllodocidae of the "Northern Bay of Bengal Ecoregion." *ZooKeys* 419, 1–27. https://doi.org/10.3897/zookeys.419.7557

Palumbi, S.R., Martin, A., Romano, S., McMillan, W.O., Stice, L., & Grabowski, G. (1991) The simple fool's guide to PCR, version 2.0. *University of Hawaii, Honolulu*, 45.

Peek, A.S., Gustafson, R.G., Lutz, R.A., & Vrijenhoek, R.C. (1997) Evolutionary relationships of deep-sea hydrothermal vent and cold-water seep clams (Bivalvia: Vesicomyidae): results from the mitochondrial cytochrome oxidase subunit I. *Marine Biology* 130, 151–61. https://doi.org/10.1007/s002270050234

Pettibone, M.H. (1989) New species of scale-worms (Polychaeta: Polynoidae) from the hydrothermal rift-area of the Mariana Back-Arc Basin in the Western Central Pacific. *Proceedings of the Biological Society of Washington*.

Pettibone, M.H. (1989) Polynoidae and Sigalionidae (Polychaeta) from the Guaymas Basin, with descriptions of two new species, and additional records from hydrothermal vents of the Galapagos Rift, 21 N, and seep-sites in the Gulf of Mexico (Florida and Louisiana). *Proceedings of the Biological Society of Washington*.

Pleijel, F. (1991) Phylogeny and classification of the Phyllodocidae (Polychaeta). *Zoologica Scripta*, 20, 225–261. https://doi.org/10.1111/j.1463-6409.1991.tb00289.x

Rodrigo, A.P., Costa, M.H., de Matos, A.P.A., Carrapiço, F., & Costa, P.M. (2015) A study on the digestive physiology of a marine polychaete (*Eulalia viridis*) through microanatomical changes of epithelia during the digestive cycle. *Microscopy and Microanalysis*, 21, 91–101. https://doi.org/10.1017/S143192761401352X

Ronquist, F., Teslenko, M., Van Der Mark, P., Ayres, D.L., Darling, A., Höhna, S., Larget, B., Liu,

L., Suchard, M.A. & Huelsenbeck, J.P. (2012) MrBayes 3.2: efficient bayesian phylogenetic inference and model choice across a large model space. *Systematic Biology*, 61, 539–42. https://doi.org/10.1093/sysbio/sys029

Rouse, G.W., & Kupriyanova, E.K. (2021) *Laminatubus* (Serpulidae, Annelida) from Eastern Pacific hydrothermal vents and methane seeps, with description of two new species. *Zootaxa*, 4915, 1–27. https://doi.org/10.11646/zootaxa.4915.1.1

Rouse, G.W., & Pleijel, F. (2003) Problems in Polychaete Systematics. *Hydrobiologia*, 496, 175–89. https://doi.org/10.1023/A:1026188630116

Rouse, G. & Pleijel, F. (2001) *Polychaetes*. OUP Oxford, 354 pp.

San Martín, G., Álvarez-Campos, P., Kondo, Y., Núñez, J., Fernández-Álamo, M.A., Pleijel, F., Goetz, F.E., Nygren, A. & Osborn, K., (2021) New symbiotic association in marine annelids: Ectoparasites of comb jellies. *Zoological Journal of the Linnean Society*, 191, 672–694. https://doi.org/10.1093/zoolinnean/zlaa034

Sibuet, M., & Olu, K. (1998) Biogeography, biodiversity and fluid dependence of deep-sea cold-seep communities at active and passive margins. *Deep-Sea Research. Part II, Topical Studies in Oceanography*, 45, 517–67. https://doi.org/10.1016/S0967-0645(97)00074-X

Smith, C.R., & Baco, A.R. (1998) Phylogenetic and functional affinities between whale-fall, seep and vent chemoautotrophic communities. *Cah Biol Mar*, 39, 345–346.

Stamatakis, A. (2014) RAxML version 8: A tool for phylogenetic analysis and post-analysis of large phylogenies. *Bioinformatics*, 30, 1312–13. https://doi.org/10.1093/bioinformatics/btu033

Stiller, J., Rousset, V., Pleijel, F., Chevaldonné, P., Vrijenhoek, R.C., & Rouse, G.W. (2013) Phylogeny, biogeography and systematics of hydrothermal vent and methane seep *Amphisamytha* (Ampharetidae, Annelida), with descriptions of three new species. *Systematics and Biodiversity*, 11, 35–65. https://doi.org/10.1080/14772000.2013.772925

Tsurumi, M., & Tunnicliffe, V. (2003) Tubeworm-associated communities at hydrothermal vents on the Juan de Fuca Ridge, Northeast Pacific. *Deep Sea Research Part I: Oceanographic Research Papers*, 50, 611–29. https://doi.org/10.1016/S0967-0637(03)00039-6

Tunnicliffe, V. (1992) The nature and origin of the modern hydrothermal vent fauna. *Palaios*, 7, 338–50. https://doi.org/10.2307/3514820

Tunnicliffe, V., Juniper, S.K. & Sibuet, M. (2003) Reducing environments of the deep-sea floor. *Ecosystems of the World*, 81–110.

Tunnicliffe, V., McArthur, A.G., & McHugh, D. (1998) A biogeographical perspective of the deep-sea hydrothermal vent fauna. *Advances in marine biology*, 34, 353–442. https://doi.org/10.1016/S0065-2881(08)60213-8

Tyler, P.A., German, C.R., Ramirez-Llodra, E., & Van Dover, C.L. (2002) Understanding the biogeography of chemosynthetic ecosystems. *Oceanologica Acta*, 25, 227–241. https://doi.org/10.1016/S0399-1784(02)01202-1

Vaidya, G., Lohman, D.J., & Meier, R. (2011) SequenceMatrix: concatenation software for the fast assembly of multi-gene datasets with character set and codon information. *Cladistics*, 27, 171–180. https://doi.org/10.1111/j.1096-0031.2010.00329.x

Van Dover, C. (2000) *The Ecology of Deep-sea Hydrothermal Vents*. Princeton University Press, 424 pp.

Van Dover, C.L. (2002) Community structure of mussel beds at deep-sea hydrothermal vents. *Marine Ecology Progress Series*, 230, 137–158. https://doi.org/10.3354/meps230137

Ward, M.E., Jenkins, C.D., & Dover, C.L.M. (2003) Functional morphology and feeding strategy of the hydrothermal-vent polychaete *Archinome rosacea* (family Archinomidae). *Canadian Journal of Zoology*, 81, 582–590. https://doi.org/10.1139/z03-034

Warèn, A., & Bouchet, P. (1989) New gastropods from East Pacific hydrothermal vents. *Zoologica Scripta*, 18, 67–102. https://doi.org/10.1111/j.1463-6409.1989.tb00124.x

Watanabe, H., Fujikura, K., Kojima, S., Miyazaki, J.I., & Fujiwara, Y. (2010) Japan: vents and seeps in close proximity. *In:* Kiel, S. (Ed.), *The Vent and Seep Biota. Vol. 33. Aspects from Microbes to Ecosystems*. Springer, Dordrecht, pp. 379–401. https://doi.org/10.1007/978-90-481-9572-5_12

Whiting, M.F., Carpenter, J.C., Wheeler, Q.D., & Wheeler, W.C. (1997) The strepsiptera problem: phylogeny of the holometabolous insect orders inferred from 18S and 28S ribosomal DNA sequences and morphology. *Systematic Biology*, 46, 1–68. https://doi.org/10.1093/sysbio/46.1.1

Wolff, T. (2005) Composition and endemism of the deep-sea hydrothermal vent fauna. *CBM-Cahiers de Biologie Marine*, 46, 97–104.

Yen, N.K., & Rouse, G.W. (2020) Phylogeny, biogeography and systematics of Pacific vent, methane seep, and whale-fall *Parougia* (Dorvilleidae: Annelida), with eight new species. *Invertebrate Systematics*, 34, 200–233. https://doi.org/10.1071/IS19042